BEST AVAILABLE IMAGES

Defective images within this document are accurate representations of the original documents submitted by the applicant.

Defects in the images may include (but are not limited to):

- BLACK BORDERS
- TEXT CUT OFF AT TOP, BOTTOM OR SIDES
- FADED TEXT
- ILLEGIBLE TEXT
- SKEWED/SLANTED IMAGES
- COLORED PHOTOS
- BLACK OR VERY BLACK AND WHITE DARK PHOTOS
- GRAY SCALE DOCUMENTS

IMAGES ARE BEST AVAILABLE COPY.

As rescanning documents *will not* correct images, please do not report the images to the Problem Image Mailbox.

Layilin, A Novel Talin-binding Transmembrane Protein Homologous with C-type Lectins, is Localized in Membrane Ruffles

Mark L. Borowsky and Richard O. Hynes

Howard Hughes Medical Institute, Center for Cancer Research and Department of Biology, Massachusetts Institute of Technology, Cambridge, Massachusetts 02139

Abstract. Changes in cell morphology and motility are mediated by the actin cytoskeleton. Recent advances in our understanding of the regulators of microfilament structure and dynamics have shed light on how these changes are controlled, and efforts continue to define all the structural and signaling components involved in these processes. The actin cytoskeleton-associated protein talin binds to integrins, vinculin, and actin. We report a new binding partner for talin that we have named layilin, which contains homology with C-type lectins, is present in numerous cell lines and tissue extracts, and is expressed on the cell surface. Layilin colocalizes with talin in membrane ruffles, and is recruited to membrane ruffles in cells induced to migrate in in vitro wounding experiments and in peripheral ruffles in spreading cells. A ten–amino acid motif in the layilin cytoplasmic domain is sufficient for talin binding. We have identified a short region within talin's amino-terminal 435 amino acids capable of binding to layilin in vitro. This region overlaps a binding site for focal adhesion kinase.

Key words: layilin • talin • ruffles • C-type lectin • focal adhesion kinase (FAK)

CELL shape and movement form the basis for fundamental developmental events such as gastrulation, tubule formation, and morphogenesis. The actin cytoskeleton plays a significant role in these processes because it is a major determinant of cell shape, and is essential for cell motility. Furthermore, interactions of actin filaments with the cell membrane are necessary both for changes in and maintenance of cell morphology. Our understanding of membrane–cytoskeleton linkages has been advanced significantly with the recognition of various proteins as adaptors between integral membrane proteins and the actin cytoskeleton. Proteins of the band 4.1 superfamily, band 4.1, talin, ezrin/radixin/moesin (ERM)[1], and merlin, the product of the neurofibromatosis type 2 tumor suppressor gene, perform this function in many cell types (Tsukita et al., 1997). Band 4.1 confers mechanical stability to red blood cells by attaching the spectrin and actin cytoskeletons to glycophorin or the erythrocyte anion exchanger (band 3) in the erythrocyte membrane (Bennett and Gilligan, 1993). Talin plays an essential role in integrin-mediated cell matrix adhesion by binding to integrin cytoplasmic domains, focal adhesion kinase (FAK), actin, and the actin-binding protein vinculin (Burridge and Mangeat, 1984; Horwitz et al., 1986; Chen et al., 1995; Hemmings et al., 1996; Knezevic et al., 1996). ERM proteins contribute to microvillar structure, function in cell adhesion, and bind to actin and sites on the plasma membrane; ERMs have been reported to bind to the cytoplasmic domains of several transmembrane proteins, including CD44, CD43, ICAM-2, and ICAM-3 (Algrain et al., 1993; Takeuchi et al., 1994; Tsukita et al., 1994; Turunen et al., 1994; Helander et al., 1996; Serrador et al., 1997; Yonemura et al., 1998).

Talin, ERMs, merlin, and band 4.1 have a similar overall domain structure, and are proposed to function by the same mechanism. They are related by sequence homology in the amino-terminal domain, which is proposed to contain their membrane-binding sites (Rees et al., 1990). ERMs can bind CD44, CD43, and ICAM-2 via their NH_2-terminal domains, and band 4.1 interacts with both glycophorin C and band 3 through its NH_2-terminal domain (Jöns and Drenckhahn, 1992; Yonemura et al., 1998). The NH_2-terminal domains of merlin and ERMs also associate with NHE-RF, which may link them indirectly to the

Address all correspondence to R.O. Hynes, Massachusetts Institute of Technology, 77 Massachusetts Avenue, E17-227, Cambridge, MA 02139. Tel.: (617) 253-6422. Fax: (617) 253-8357. E-mail: rohynes@mit.edu

1. *Abbreviations used in this paper*: CRD, carbohydrate-recognition domains; ERM, ezrin/radixin/moesin; GST, glutathione-S-transferase; nt, nucleotide.

membrane by binding to one or more Na^+-H^+ exchanger isoforms (Reczek et al., 1997; Murthy et al., 1998). In addition to the sequence homology in their NH_2-terminal domains, talin and ERMs have a central domain predicted to be mostly α-helical and demonstrating actin-binding activity, while this region of band 4.1 binds spectrin (Ungewickell et al., 1979; Rees et al., 1990; McLachlan et al., 1994). With these biochemical activities, band 4.1 family members could link membrane and cytoskeleton by binding to each simultaneously.

Talin, which is expressed in essentially all adherent cell types, is found at sites of cell-matrix adhesion (such as focal contacts), leading edge ruffles of migratory cells, at sites of phagocytosis in macrophages, and at cell–cell contacts of T cells (Burridge and Connell, 1983; Burn et al., 1988; Greenberg et al., 1990; DePasquale and Izzard, 1991; Kreitmeier et al., 1995). These are also sites where integrin cell adhesion receptors are found. While integrins are clearly associated with the leading edge of some types of motile cells, it is unclear whether they are located in dorsal ruffling membrane sheets, in the ventral-most base of the leading edge, or both (Schmidt et al., 1993; Lawson and Maxfield, 1995; Lee and Jacobson, 1997). Talin's importance in adhesion and migration has been demonstrated in experiments that interfere with talin function or expression. Injection of anti-talin antibodies disrupts cell adhesion and migration, and downregulation of talin protein levels by expression of anti-sense talin RNA reduces the rate of cell spreading (Nuckolls et al., 1992; Albigès-Rizo et al., 1995). Talin's role as a membrane–cytoskeleton linker in focal contacts has been characterized in detail; a short peptide derived from the β1-integrin cytoplasmic domain can block the association of talin with integrins, and three actin-binding domains and three vinculin-binding sites have been mapped in talin (Tapley et al., 1989; Hemmings et al., 1996). Interestingly, the integrin-, three vinculin-, and two of the three actin-binding sites in talin are all found within the carboxy-terminal 190-kD calpain tail fragment of talin (Horwitz et al., 1986; Gilmore et al., 1993; Hemmings et al., 1996). Microinjected talin tail fragment localizes to focal contacts, suggesting that the known integrin-, vinculin-, and actin-binding sites account for talin's membrane–cytoskeleton linking role in focal contacts (Nuckolls et al., 1990). In contrast, talin's role in membrane ruffles has not been elucidated, although it seems reasonable to project that, as in focal contacts, it connects F-actin to an unknown site on the plasma membrane.

While the tail fragment can account for talin's role in focal adhesions, the role of talin's 47-kD amino-terminal calpain cleavage product (talin head, amino acids 1–435) is not known. An examination of talin protein sequence from highly divergent organisms reveals that talin's NH_2-terminal domain is the most well-conserved region within the sequence. For instance, *Caenorhabditis elegans* and *Dictyostelium discoideum* talins are 78 and 66% similar to mouse talin within the head domain, but only 59 and 46% similar to mouse talin overall (Kreitmeier et al., 1995; Moulder et al., 1996). This highly conserved segment also contains talin's homology to band 4.1. While this sequence conservation suggests that some conserved function exists for the talin head domain, experimental analyses have given varied results. Nuckolls et al. found that a small fraction of microinjected talin 47-kD domain fragment incorporated into focal contacts, while most was diffusely localized in cells. The injected protein had no effect on cytoskeletal morphology, cell spreading, or adhesion. However, injected talin tail protein was targeted to focal contacts, and also exhibited ectopic localization at cell–cell junctions where full-length talin is not normally found, suggesting that talin head may enhance targeting to focal contacts or mask other binding sites within talin's tail domain (Nuckolls et al., 1990). In contrast, microinjected glutathione-S-transferase (GST)-talin 47-kD fragment colocalized with actin filaments and disrupted stress fibers in a majority of cells (Hemmings et al., 1996). Similarly, we found that cells transiently overexpressing talin head were not spread and appeared poorly adherent (M.L. Borowsky and R.O. Hynes, unpublished results). Bolton and colleagues generated two anti-talin monoclonal antibodies that, when microinjected into human foreskin fibroblasts, disrupt actin stress fibers, and when injected into chick embryo fibroblasts, significantly inhibit cell migration (Bolton et al., 1997). One of these monoclonal antibodies recognizes an epitope in the talin 47-kD fragment, and the other binds a site at the extreme COOH terminus of talin.

While the talin head domain appears to play an important role in cell motility and morphology, no specific mechanism has been proposed to explain these observations. Based on the sequence similarity between talin's NH_2-terminal domain and band 4.1, we hypothesized that the conserved talin head domain contained an additional membrane-binding site for talin. In a two-hybrid screen we have identified a previously unknown type I integral membrane protein that interacts with talin head, is expressed in all adherent cell lines analyzed, and colocalizes with talin in membrane ruffles. A short motif present in the cytoplasmic domain of this protein is sufficient for talin head binding. We believe this protein represents a membrane-binding site for talin in ruffles, while integrins anchor talin in focal contacts.

Materials and Methods

Yeast Two-hybrid Screen

Plasmid construction. Manipulation of DNA was performed according to standard molecular biological protocols (Sambrook et al., 1989). Unless otherwise stated, restriction enzymes and DNA-modifying enzymes were purchased from New England Biolabs Inc. (Beverly, MA). A pBluescript subclone of a talin cDNA encoding amino acids 1–435 (clone A14) was made by partially digesting a chicken talin cDNA with NcoI, digesting with PstI, and cloning the product into pBluescript SK- that had been digested with NcoI and PstI. To make the LexA fusion bait, clone A14 was digested with SacI and EcoRV, the ends were polished with T4 DNA polymerase, and the appropriate fragment was ligated into pEG202 that had been digested with EcoRI and rendered blunt (Gyuris et al., 1993). A pJG4-5 subclone of layilin lacking a cytoplasmic domain was made by inserting a synthetic oligonucleotide (2STOPS: CGGTTAATGATCATTAACCG) with two in-frame stop codons into the 3′ PvuII site in the longest partial layilin cDNA isolated in the two-hybrid screen (Gyuris et al., 1993). A pJG4-5 subclone of layilin cytoplasmic domain was made by ligating a PvuII/XhoI layilin cDNA fragment into pJG4-5 that had been digested with EcoRI, Klenow-blunted, and digested with XhoI. A plasmid encoding LexA fused to the type-II TGFβR cytoplasmic domain was the gift of Dr. R. Weinberg (Massachusetts Institute of Technology).

Library screen. The two-hybrid library screen was performed as previously described using the CHO cDNA library pVPCHO (gift of Dr. V.

Prasad, Albert Einstein Medical College; Gyuris et al., 1993). EGY48 containing the LexA-talin bait and the beta-galactosidase (β-gal) reporter plasmid pSH18-34 was transformed with DNA prepared from two pools of pVPCHO library that contained ~7.5 × 10^4 and 8.2 × 10^4 recombinants. Yeast transformants were pooled and frozen in aliquots, and their plating efficiency was determined. About 10^6 yeast transformants were plated on synthetic complete medium containing raffinose and galactose as carbon sources, but lacking histidine, leucine, tryptophan, and uracil. 48–96 h later, 244 yeast colonies were picked and assayed for blue color on medium containing X-gal (Boehringer Mannheim Corp., Indianapolis, IN). Plasmid DNA was recovered from 40 double-positive (leu^+, $lacZ^+$) colonies, and candidate interactors were sorted into classes based on AluI and HaeIII restriction digestion patterns of the library inserts (Hoffman and Winston, 1987; Gyuris et al., 1993). After retesting representative interactors of each class with negative control baits, 30 of the original 40 clones were deemed worthy of further study. Based on partial sequence data, these 30 candidates were determined to comprise three cDNAs (Epicentre PCR sequencing kit, Epicentre Technologies, Madison, WI).

Anchored PCR. Primers internal to the longest layilin cDNA recovered from pVPCHO (LECTF1: TGGACAGATGGGAGCACAT; and LECTR1: GGAATTCCCCACTTTCTGAAGGGTTC) were used to screen pools of a CHO cDNA library subcloned in pcDNA I (gift of Dr. M. Krieger, Massachusetts Insititute of Technology) for the presence of our interactor cDNA (Guo et al., 1994). A fragment of the layilin cDNA was amplified from a positive pool using a 3′ primer within the cDNA (LECTR1), and a 5′ primer complementary to the T7 promoter present in the vector (T7P: TAATACGACTCACTATAGG), subcloned into pBluescript, sequenced, and found to encode an open reading frame continuous with and overlapping that in the cDNA cloned from pVPCHO. The open reading frame encoded by the PCR product completed the C-type lectin homology present in the original pVPCHO isolate, contained a suitable start codon, and so was deemed likely to be the genuine 5′ end of the cDNA.

Northern analysis. CHO RNA was prepared by acid phenol extraction as previously described (Chomczynski and Sacchi, 1987) Poly-A^+ RNA was isolated essentially as described (Bradley et al., 1988). In brief, 20 × 15-cm dishes of nearly confluent CHO cells were trypsinized, pooled, pelleted, and washed with PBS. The cells were resuspended in 20 ml of proteinase K solution (200 μg/ml proteinase K, 0.5% SDS, 100 mM NaCl, 20 mM Tris, pH 7.5, 1 mM EDTA), lysed with 3× 25-s cycles in a Polytron homogenizer (Brinkmann Instruments, Waterbury, NY), and incubated for 90 min at 37°C. The NaCl concentration was brought to 500 mM, and 200 mg of oligo dT cellulose (as a suspension in high salt buffer [0.1% SDS, 500 mM NaCl, 20 mM Tris, pH 7.5, 1 mM EDTA]; Pharmacia Biotech, Inc., Piscataway, NJ) was added per 10^9 cells. After mixing for 2 h at room temperature, the oligo dT cellulose was washed twice in batch with high-salt buffer, and was poured as a column in a 1-ml syringe plugged at the bottom with sterile glass wool. The resulting column was washed with 10-column volumes of high-salt buffer and then eluted with 4-column bed volumes of low salt buffer (0.05% SDS, 20 mM Tris pH 7.5, 1 mM EDTA). The four fractions were pooled, heated to 65°C for 5 min, cooled on ice, brought to a final NaCl concentration of 0.5 M, and incubated with a fresh aliquot of oligo dT cellulose for 30 min at RT. Washes, column building, elutions, and rebinding were repeated as above twice for a total of three rounds of selection on oligo dT cellulose. On the last cycle, four 300-μl fractions of poly-A^+ RNA were eluted in low-salt buffer and ethanol-precipitated overnight at −20°C. RNA was pelleted, washed with 70% ethanol, and resuspended in 50 μl of diethylpyrocarbonate-treated water. Samples were electrophoresed on 1% agarose/formaldehyde gels, transferred to Hybond-N nitrocellulose (Amersham Life Science, Inc., Arlington Heights, IL), cross-linked in a Stratagene stratalinker (Stratagene, La Jolla, CA), prehybridized for 2 h at 57.5°C in Church-Gilbert buffer (1 mM EDTA, 500 mM Na_2HPO_4 pH 7.2, 7% SDS, 1% BSA), hybridized overnight at 57.5°C in Church-Gilbert buffer containing 10^6 cpm of random-primed layilin probe, washed twice at room temperature in 2× SSC/0.1% SDS and twice at 55°C in 0.2× SSC/0.1% SDS, and then exposed on X-OMAT AR film (Eastman Kodak Co., Rochester, NY) with an intensifying screen at −80°C (Alwine et al., 1977).

Preparation of Polyclonal Anti-layilin Antisera

A synthetic oligopeptide consisting of a cysteine followed by the carboxy-terminal 20 amino acids of layilin (LC20: CSPDRMGRSKESGWVENEIYY) was purchased from the Massachusetts Institute of Technology Biopolymer Facility, conjugated to keyhole limpet hemocyanin as previously described, and sent to Covance (Denver, PA) for production of rabbit antisera (Marcantonio and Hynes, 1988).

Affinity purification. A thiopropyl-Sepharose 6B (Pharmacia Biotech, Inc.) column with covalently-coupled LC20 was washed sequentially with 15 ml of 10 mM Tris, pH 7.5 under gravity flow, 100 mM glycine, pH 2.5 at 25 ml/h, 10 mM Tris, pH 7.5 at 25 ml/h. Ammonium sulphate–precipitated antiserum was applied to the column at 20 ml/h. The flow rate was increased to 25 ml/h, and the eluate recirculated on the column for 30 min so that the antiserum ran over the column a total of three times. On the last cycle, the depleted serum was collected and saved for use as a control for the affinity-purified antiserum. The column was washed at 25 ml/h with 30 ml of 10 mM Tris pH 7.5, and then at 30 ml of 500 mM NaCl in 10 mM Tris pH 7.5. Antibody was eluted in 1.2-ml fractions with 100 mM glycine pH 2.5 into 1.5-ml microcentrifuge tubes preloaded with 1 M Tris, pH 8.0 sufficient to neutralise the glycine.

GST Fusion Binding

Plasmid construction. The GST-chicken talin 1-435 fusion (GST-CT) was made by ligating a BamHI/EcoRI fragment from chicken talin clone A14 into BamHI/EcoRI-digested pGEX-2T (Pharmacia Biotech Inc.). Deletions within this region of talin were made by either digesting this construct with appropriate enzymes, or by generating PCR products within it. Specifically, to make GST-CT 280-435, GST-CT was cut with BglII and BamHI, blunted with Klenow, and religated. To generate GST-CT 1-280, GST-CT was cut with BglII and EcoRI, blunted with Klenow, and religated. To create GST-CT 186-435, GST-CT was cut with ClaI and BamHI, blunted with Klenow, and religated. The insert for GST-CT 186-357 was derived from GST-CT 186-435 using PCR with a primer starting at the codon for amino acid 357 (CTR1: CGAATTCGATGTTGGTCAGGCTCC) and a primer in the vector (pGEX1: TTGCAGGGCTGGCAAGC). The insert for GST-CT 225-435 was synthesized by PCR using a primer starting at the codon for amino acid 225 (CTF1: CGGATCCGGCTCCCACCCCGTC) and a primer in the vector (pGEX2: GCTGCATGTGTCAGAGG). A PCR product encoding amino acids 225–357 was produced using the primers CTF1 and CTR1. Each PCR product was digested with BamHI and EcoRI and ligated into BamHI/EcoRI-digested pGEX-2T. To make the GST-layilin cytoplasmic domain fusion containing amino acids 261–374, a pBluescript subclone of layilin cDNA was made that extends from the 3′ XhoII site to the 3′ end of the cDNA, with the XhoII site blunted and ligated to the pBluescript EcoRV site, and the 3′ end of the layilin cDNA cloned into the pBluescript XhoI site. The construct was digested with EcoRI and XhoI, and the appropriate fragment was cloned into EcoRI/XhoI-cut pGEX-5X-1 (Pharmacia Biotech Inc.). The GST-layilin 244–335 fusion was made by amplifying the cDNA encoding those amino acids with primers LECTF2 (GGAATTCTCAGCTGCATGTTGGGTT) and LECTR1, digesting the PCR product with EcoRI, and subcloning the fragment into EcoRI-digested, phosphatase-treated pGEX-5X-1. The GST-layilin 330–374 fusion was made by amplifying a pBluescript subclone of the layilin cDNA with a 5′ primer starting with the codon for amino acid 330 (LECTF3: GGAATTCAACCCTTCAGAAAGTGGGTT) and T7P. The PCR product was digested with EcoRI and XhoI, and the resulting fragment was ligated into pGEX-5X-1 that had been digested with EcoRI and XhoI. The GST-(LH23)×3 fusion was made by self-ligation of a double-stranded oligomer consisting of top-strand LH23T (GATCCTTGAGAGTGGATTTGTGACCAATGACATTTATGA) and bottom-strand LH23B (GATCTCATAAATGTCATTGGTCACAAATCCACTCTCAAG), digestion with BamHI and BglII, and ligation of the resulting multimerized oligomer into pGEX-5X-1 that had been digested with BamHI and treated with shrimp alkaline phosphatase (Boehringer Mannheim Corp.). All GST-talin and GST-layilin fusion protein constructs were confirmed by sequence analysis. The GST-fibronectin (FN) EIIIB construct has been previously described (Peters et al., 1995).

Affinity isolation. Detergent lysates of CHO, NIL8, or their transfected derivatives were made by scraping and pooling cells, washing with Tris wash buffer (50 mM Tris, pH 7.5, 150 mM NaCl, 1 mM $MgCl_2$, 1 mM $CaCl_2$), and then lysing on ice for 20 min with 1 ml of lysis buffer (0.1% TX-100, 0.3 M sucrose, 50 mM Tris, pH 7.5, 100 mM KCl, 1 mM $CaCl_2$, 2.5 mM $MgCl_2$, 1 mM PMSF, 9 TIU/ml aprotinin, 5 μg/ml leupeptin) per 10^7 cells. The lysate was centrifuged at 13,000 *g* for 10 min at 4°C, and was then precleared with 500 μl of packed glutathione-agarose (preequilibrated in lysis buffer) per ml of lysate for 30 min at 4°C. For peptide-blocking experiments, 5 mg/ml peptide in PBS was added to a final concentration of 1 mg/ml to the cleared lysate, and the mixture was incubated on ice for 20 min. 500 μl of cleared lysate was added to 50 μl of glutathione-agarose preloaded with each GST-fusion protein, and was ro-

tated end-over-end for 1 h at 4°C. The samples were centrifuged briefly, the supernatants were removed, and the glutathione-agarose pellets were washed four times with 500 μl lysis buffer without detergent. The glutathione-agarose pellets were then boiled for 10 min in an equal volume of 1× gel loading buffer, and were analyzed by Western blotting (Towbin et al., 1979).

Preparation of Tissue Lysates

Organs dissected from an adult female mouse were washed twice with cold PBS, resuspended in an equal volume of homogenization buffer (100 mM NaCl, 10 mM Tris, pH 7.5, 1 mM EDTA, 1 mM PMSF, 9 TIU/ml aprotinin, 5 μg/ml leupeptin), and homogenized on ice with an electric grinder (Kontes, Vineland, NJ) in 1.5-ml microcentrifuge tubes. An equal volume of 2× RIPA buffer (1× RIPA: 1% Triton X-100, 1% sodium deoxycholate, 0.1% SDS, 158 mM NaCl, 10 mM Tris, pH 7.5, 1 mM EGTA, 1 mM PMSF, 9 TIU/ml aprotinin, 5 μg/ml leupeptin) was added, and samples were vortexed, incubated on ice for 60 min, boiled for 10 min, spun at 13,000 *g* at 4°C for 10 min, and assayed for total protein using a detergent-compatible protein assay (Bio-Rad Laboratories, Hercules, CA). An equal mass of each sample was analyzed by Western blotting.

Avidin Depletion

Three 10-cm dishes of nearly confluent CHO cells (10^7 cells) were washed with PBS, and cells were released with versene (0.02% EDTA, PBS, phenol red), pooled, washed twice with PBS, and diluted to a density of 5×10^6/ml with PBS. The sample was divided into two parts, and DMSO containing 10 mg/ml EZ-Link sulfo-NHS-LC-biotin (Pierce Chemical Co., Rockford, IL) was added to one half of the sample while DMSO alone was added to the other half, and cells were rocked gently for 60 min at room temperature (Isberg and Leong, 1990). Cells were washed three times with 1 ml of Tris wash buffer, lysed in 1.5 ml RIPA buffer, sheared through a 26-gauge needle to reduce viscosity, and spun for 10 min at 4°C and 13,000 *g* to remove insoluble debris. Two 1-ml syringes plugged with glass wool were packed with 200 μl of Immunopure Immobilized Monomeric Avidin (Pierce Chemical Co.), poured as a 33% slurry, and prepared according to the manufacturer's instructions. The columns were loaded with 200 μl of biotin-labeled or mock-labeled lysate and capped and incubated at room temperature for 76 min, and then PBS was applied to each column as three 200-μl fractions were collected. Equal volumes of each eluted fraction were analyzed by Western blotting.

Surface Labeling and Immunoprecipitation

RIPA lysates from surface-biotinylated CHO cells were prepared as described above. Lysate from 8×10^5 cells was mixed with 50 μl of protein A Sepharose CL-4B (as a 1:1 slurry in RIPA buffer; Pharmacia Biotech Inc.), 1 μl of anti-layilin antiserum or control serum, and 1 mg of heat-inactivated BSA in RIPA buffer in a total volume of 450 μl. After incubating at 4°C overnight with end-over-end mixing, the Sepharose was washed five times with 1 ml RIPA buffer. Each sample was divided into two parts, and one part was treated with peptide N-glycosidase F (PNGase F) according to the manufacturer's instructions (New England Biolabs Inc.). Samples were boiled for 10 min in 1× gel loading buffer, spun for 10 min at 13,000 *g* at room temperature, electrophoresed on 7.5% acrylamide gels, and transferred to nitrocellulose filters. Filters were blocked overnight at 4°C in blocking buffer (5% non-fat dry milk reconstituted in PBS/0.1% Tween-20), rinsed twice, and then washed once for 5 min with PBS/0.1% Tween-20, incubated for 45 min at room temperature with HRP-streptavidin (Amersham Life Science, Inc., Arlington Heights, IL) diluted 1:2,000 in PBS/0.1% Tween-20, rinsed twice, and then washed once for 15 min in PBS/0.1% Tween-20, followed by 5 × 10-min washes in PBS/0.1% Tween-20. Bands were detected using chemiluminescence (NEN™ Life Science Products, Boston, MA).

Generation of Cell Lines Expressing Epitope-tagged Layilin

A hemagglutinin (HA)-tagged version of layilin was made by inserting a synthetic EcoRI linker (New England Biolabs Inc.) into the 5′ PvuII site in the layilin cDNA. An oligonucleotide encoding the sequence EFYPYDVPDYASPEF was ligated into the EcoRI linkered form of layilin, and this construct was confirmed by DNA sequencing (Wilson et al., 1984). The tagged layilin cDNA was transferred into the expression vector pLEN-neo, and the resulting construct transfected into cells using standard calcium-phosphate protocols.

Immunofluorescence

Adherent NIL8 cells were released with trypsin/EDTA, plated on glass coverslips coated with 5 μg/ml human plasma fibronectin (Beckton Dickinson, Bedford, MA), and incubated for 15 min to detect ruffles in spreading cells, overnight to obtain well-spread cells, or several days to achieve high cell density for in vitro wounding experiments. Spreading cells were stained before fixation and permeabilization, although identical staining patterns were observed when staining was performed on fixed and permeabilized cells. Otherwise, cells were stained after fixation and permeabilization as follows. Coverslips were washed three times in PBS, fixed for 10 min in 4% paraformaldehyde in PBS, washed as above, permeabilized for 10 min in 1% Brij 99 (Fluka, Ronkonkoma, NY) in PBS, washed as above, blocked with 10% normal goat serum (NGS, Vector Labs, Inc., Burlingame, CA) in PBS for 30 min at 37°C, incubated with primary antibody diluted in 10% NGS/PBS for 30 min at 37°C, washed as above, incubated with fluorescently labeled secondary antibodies (Biosource International, Camarillo, CA), and fluorescently labeled phalloidin (Sigma Chemical Co.) as appropriate for 30 min at 37°C, washed as above, rinsed once in water, and mounted in gelvatol (Monsanto, St. Louis, MO) containing DABCO (Sigma Chemical Co.) to prevent fading. For peptide-blocking experiments, antibodies were preincubated on ice with an appropriate peptide at 1 mg/ml for at least 30 min. Antibodies were used at the following dilutions: anti-layilin, 1:200; TD77 (anti-talin), 1:100; 12CA5 (anti-HA-tag), 1:2,000; secondary antibodies, 1:200; phalloidin, 1:5,000. Monoclonal antibody TD77 was the gift of Dr. D.R. Critchley, University of Leicester (Bolton et al., 1997). Stained cells were viewed on a Zeiss Axiophot, and immunofluorescent images were recorded on film (Eastman Kodak Co., Rochester, NY) except for Fig. 7, *g*, *h*, and *i*, which were recorded digitally on an Axioplan 2 (Carl Zeiss Inc., Thornwood, NY) equipped with a CCD camera (Photometrics, Tucson, AZ) and IPLab Spectrum software (Signal Analytics, Vienna, VA). For wounding experiments, confluent monolayers grown on fibronectin-coated coverslips were scraped under warm PBS with a rubber policeman to remove approximately half of the monolayer, and were then returned to a 37°C/5% CO_2 incubator for 45–90 min until prominent phase-dark ruffles were observed (Nuckolls et al., 1992).

Results

Identification of a Talin-head-binding Partner by a Yeast Two-hybrid Screen

Given talin's homology to other members of the band 4.1 superfamily, we hypothesized that talin's NH_2-terminal domain, like those of band 4.1 and ERM proteins, would bind to an integral membrane protein. Since previous biochemical efforts to find such a talin-head-binding protein yielded no candidates, we used a LexA-based yeast two-hybrid system to find talin-head-binding proteins (our unpublished results; Nuckolls et al., 1990; Gyuris et al., 1993). We generated a LexA-talin fusion protein containing the band 4.1-homologous region of chicken talin (amino acids 1–435). This fusion protein is expressed in yeast, and neither alone nor when coexpressed with the B42 acidic transcriptional activator, activated either the leu2 or β-gal reporter genes (data not shown). In a yeast transciptional repression assay we found that the LexA-talin fusion protein downregulates reporter gene expression by fourfold, indicating that our talin bait enters the nucleus and binds to LexA binding sites (Gyuris et al., 1993; data not shown). We screened approximately 10^6 yeast colonies representing about 10^5 cDNAs from a CHO cDNA library with this LexA-talin head bait, and picked 40 colonies that displayed both leucine prototrophy and the ability to activate a lacZ reporter. After grouping the 40 cDNAs into classes based on Alu and HaeIII restriction patterns, we recov-

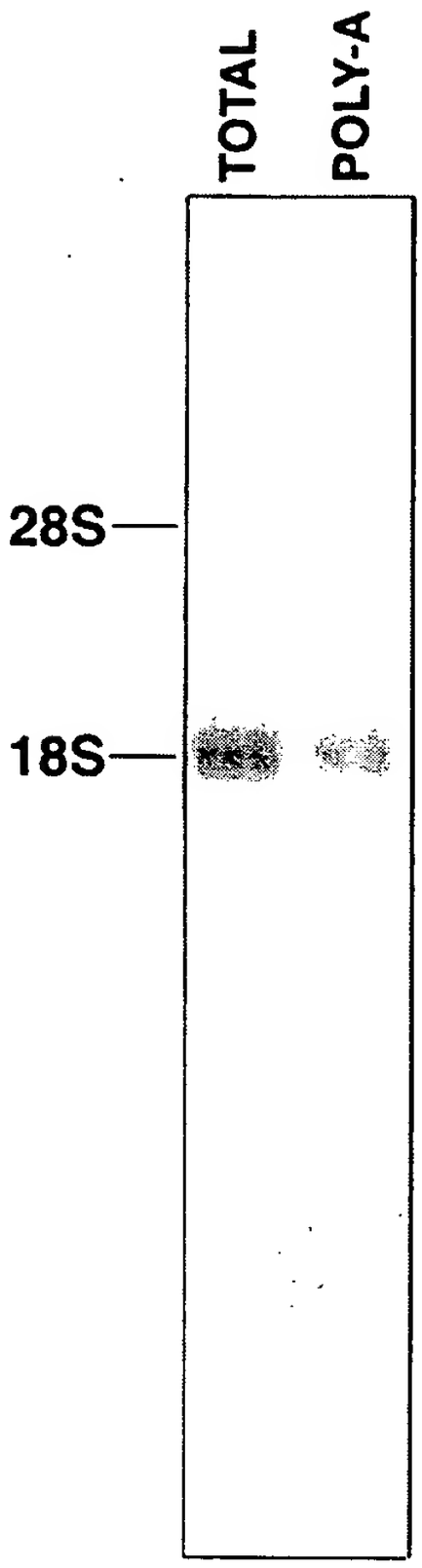

Figure 1. Northern blot analysis of CHO total and poly-A$^+$ RNA. 5 μg of CHO total RNA or 1 μg of CHO poly-A$^+$ RNA were analyzed for expression of a gene encoding a candidate talin-interacting protein. The single detectable transcript is highly enriched in the poly-A$^+$ RNA. The lane showing total RNA was exposed for 15 d and that showing poly-A$^+$ RNA for 2 d. The positions of the 18S (1874 nt) and 28S (4718 nt) ribosomal RNAs are indicated for size reference.

ered representative cDNAs from each class and retested them with the LexA-talin-head bait and a panel of four negative control LexA-fusion protein baits (LexA-max, LexA-bicoid, LexA-sec16p, LexA-TGFβR; Zervos et al., 1993; Espenshade et al., 1995). We recovered 30 cDNAs comprising a total of three genes that reproduced leucine prototrophy and β-gal activation when cotransformed into yeast with the talin bait, but not with the negative controls. Of these 30 cDNAs, 25 were overlapping fragments of a previously unidentified cDNA. We cloned the 5′ end of the cDNA encoding this candidate talin-interacting protein from a pcDNA-CHO library using anchored PCR with a primer based on our novel cDNA (Guo et al., 1994). Probes derived from the resulting 1,747-bp cDNA detected a single 1,800 nucleotide (nt) band in CHO RNA (Fig. 1).

The cDNA contains an open reading frame predicted to encode a 374–amino acid protein of an estimated molecular mass of 43 kD (Fig. 2 *a*). The protein has an amino-terminal signal sequence and predicted cleavage site typical of a secreted or transmembrane protein, a 130–amino acid domain with significant homology to C-type lectin carbohydrate-recognition domains (CRD), a 30–amino acid hydrophobic span suggestive of a transmembrane domain, and a 120–amino acid COOH-terminal domain containing three novel repeated motifs and two YXXΦ motifs similar to those known to allow AP-2–mediated recycling of some transmembrane proteins (von Heijne, 1986; Letourneur and Klausner, 1992; Drickamer, 1993). We named this protein *layilin* based on the sequence LAYILI found in its putative transmembrane domain.

Since talin is a cytosolic protein, a physiologically relevant interaction between layilin and talin must be mediated by layilin's putative cytoplasmic domain. Each of the seven independent layilin cDNAs recovered and sequenced contains the cytoplasmic domain of layilin, suggesting that the layilin cytoplasmic domain is sufficient for talin binding. We confirmed this by testing the cytoplasmic domain and the extracellular and transmembrane domains separately in the two-hybrid assay. The layilin cytoplasmic domain alone (amino acids 244–374) conferred leucine prototrophy and activated the LacZ reporter whereas the largest B42-fusion, which contains most of the rest of layilin (amino acids 92–244), did not (data not shown).

A comparison of layilin's C-type lectin homologous sequences with the CRDs of two known C-type lectins is shown in Fig. 2 *b*. Layilin contains 14/14 residues found in all carbohydrate-binding C-type lectins, and an additional 18/20 highly conserved residues (Drickamer, 1993). One of the two nonconserved residues, V141, corresponds to an oxygen-containing residue that coordinates one of two calcium ions bound by some C-type lectins (Weis et al., 1991). However, not all lectins use this calcium-binding site, and the absence of an oxygen-containing side chain at position 141 suggests that layilin lacks this second calcium-binding site (Graves et al., 1994). Interestingly, layilin contains a 5–amino acid insertion relative to the mannose-binding protein CRD (amino acids 148–152 of layilin; Fig. 2 *b*, *underline*), which is of the same size and at the identical position as an insertion found in the E-selectin CRD. The inserted sequences in the E-selectin CRD form a loop that projects into the ligand-binding pocket, and mutation of these sequences disrupts selectin-mediated adhesion (Graves et al., 1994). Layilin contains an additional 7–amino acid insertion adjacent to the 5–amino acid insertion that may form part of the same loop (Fig. 2 *b*, *double underline*). Layilin shares ~40% amino acid similarity with all other CRDs examined; the presence of a selectin-like insertion raises the possibility that layilin may bind to ligand in a manner similar to selectins. Layilin also differs from other CRDs by inserting 7 amino acids relative to the mannose-binding protein CRD (amino acids 102–108 of layilin, Fig. 2 *b*, *broken underline*). This insertion falls in sequences that form the first of four large calcium-binding loops in other CRDs, and is distal to the proposed ligand-binding, site. The 45 amino acids between the CRD and the putative transmembrane domain are rich in negatively charged amino acids (11/45), prolines (7/45), and S/T residues that may serve as O-linked carbohydrate attachment sites (10/45). These characteristics are suggestive of an elongated stalk that projects the CRD away from the plasma membrane.

Potential human and pig layilin homologues present in the expressed sequence tag (EST) database indicate con-

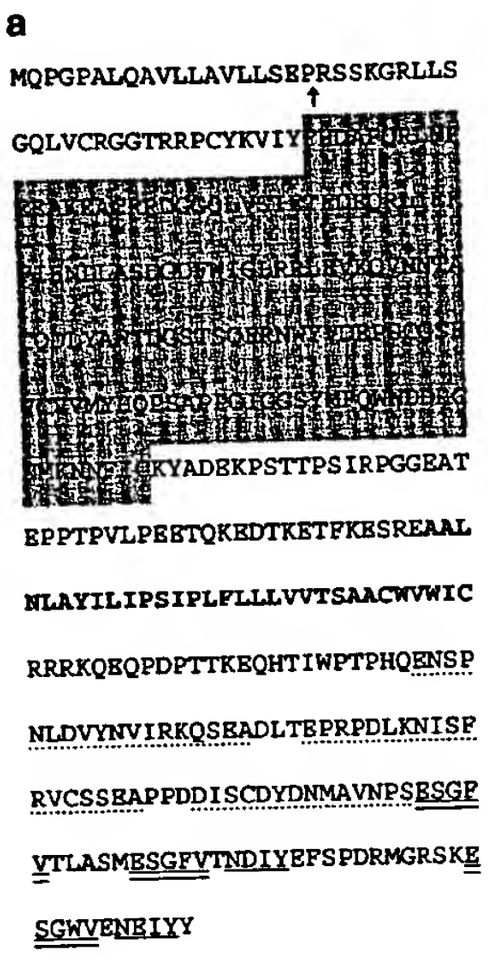

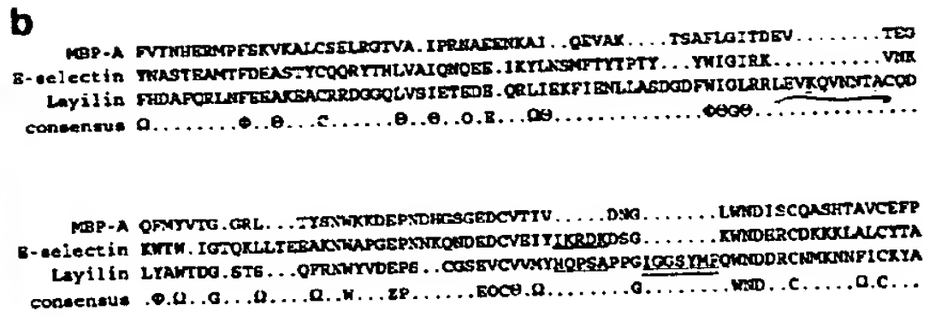

Figure 2. (*a*) The deduced layilin amino acid sequence is shown. The predicted signal sequence cleavage site is indicated with an arrow. A grey box highlights the C-type lectin homology. A single potential N-linked glycosylation site is marked with a diamond. The proposed transmembrane domain is shown in boldface. Three copies of a 16–18 amino acid repeat (layilin homology 1, LH1) are shown with a broken underline. Three copies of a penta-amino acid repeat (LH2) are double-underlined, and two copies of a tetra-amino acid repeat (LH3) are underlined. The cDNA encoding this polypeptide has been submitted to GenBank with accession number AF093673. (*b*) Alignment of the carbohydrate-recognition domains from rat mannose-binding protein A, dog E-selectin, and hamster layilin. Shown at the bottom is the CRD consensus sequence derived by Drickamer (1993): single-letter amino acid code indicates absolutely conserved residues; other abbreviations: O, any oxygen-containing amino acid; Z, either E or Q; θ, aliphatic; Φ, aromatic; Ω, aliphatic or aromatic residue (Drickamer, 1993). The alignment was performed using the GCG program PILEUP, and was then manually adjusted. The five amino acid insertions found in layilin and E-selectin are underlined, a 7–amino acid insertion unique to layilin is double-underlined, a second 7–amino acid insertion is shown with a broken underline.

servation among different species of some layilin sequence features. First, the pig EST (accession no. AA063669) encodes a protein that includes most of the layilin CRD. This potential homologue is 80% identical and 88% similar to hamster layilin, and includes the insertions discussed above. In addition, both hamster and pig layilin sequences contain the sequence EPS in a motif that has some value in predicting the carbohydrate specificity of CRDs; CRDs containing the sequence EPN generally bind mannose or glucose while those with the sequence QPD tend to bind galactose sugars (Drickamer, 1992). We cannot make any prediction based on the sequence EPS found in layilin. The second candidate layilin homologue is encoded by two human ESTs (accession nos. AA447940 and AA384314), and overlaps the layilin cytoplasmic domain. The 92–amino acid hypothetical human protein is 73% identical and 83% similar to hamster layilin, and contains three copies of the long repeat and a single copy of each of the short cytoplasmic domain motifs. Alignment of the human and hamster cytoplasmic domains reveals that the human version lacks the COOH-terminal 20 amino acids, precisely those used in our peptide antigen. This may explain our inability to detect layilin protein in human cell lines with our antibody (see below).

Layilin Protein is Widely Expressed in Cells and Tissues

We raised a polyclonal antiserum directed against a keyhole limpet hemocyanin-conjugated peptide corresponding to the 20 carboxy-terminal amino acids of layilin, and affinity-purified it against the immobilized peptide. Both the serum and affinity-purified antibodies detect a cluster of bands migrating at ~55 kD in detergent lysates of CHO cells, while the serum depleted over the peptide column did not detect any specific bands (Fig. 3 *a*, compare lanes *3* and *5* with lane *4*). Fig. 3 *a* also shows that the bands detected by the anti-layilin antiserum are competed by the layilin-derived peptide (compare lane *1* with lane *2*). In cells transfected with an HA-tagged layilin cDNA, the anti-HA monoclonal antibody 12CA5 detects a similar cluster of bands that migrate slightly more slowly, presumably because of the presence of the HA tag; the anti-layilin antiserum detects the same bands (data not shown).

To find out whether layilin, like talin, is expressed in a variety of cell lines and cell types, we screened several cultured cell lines and mouse tissues for the presence of layilin protein. Our antiserum detected an immunoreactive protein of approximately the same size as hamster layilin in each cell line tested, except the human cell line K562 (Fig. 3 *b*). These bands were efficiently competed in the presence of the layilin-derived peptide LC20 (data not shown). The cross-reacting band in three rat cell lines tested migrated slightly faster than the band in hamster cell lysates, indicating a molecular weight difference of ~4 kD. This result could represent differential glycosylation (see below) or a deletion or alteration in the polypeptide itself. We observed a significantly weaker signal in COS cells, indicating either that these cells express less layilin protein or that the monkey antigen does not cross-react with our antibody as well as rodent layilins. Our inability to detect layilin-reactive protein in human cells might be explained by the sequence of the candidate human layilin homologue described above. We found detectable levels of layilin in most of the 12 mouse tissues analyzed by Western blotting (Fig. 3 *c*). Layilin was most abundant in the ovary, and was readily detectable in most other solid tissues assayed. These observations indicate that layilin, like talin, is widely expressed in adherent cell types both in vitro and in vivo.

GST-talin-head Fusions Bind Layilin and FAK

To confirm and characterize further the interaction between talin and layilin, we tested the ability of GST fusion

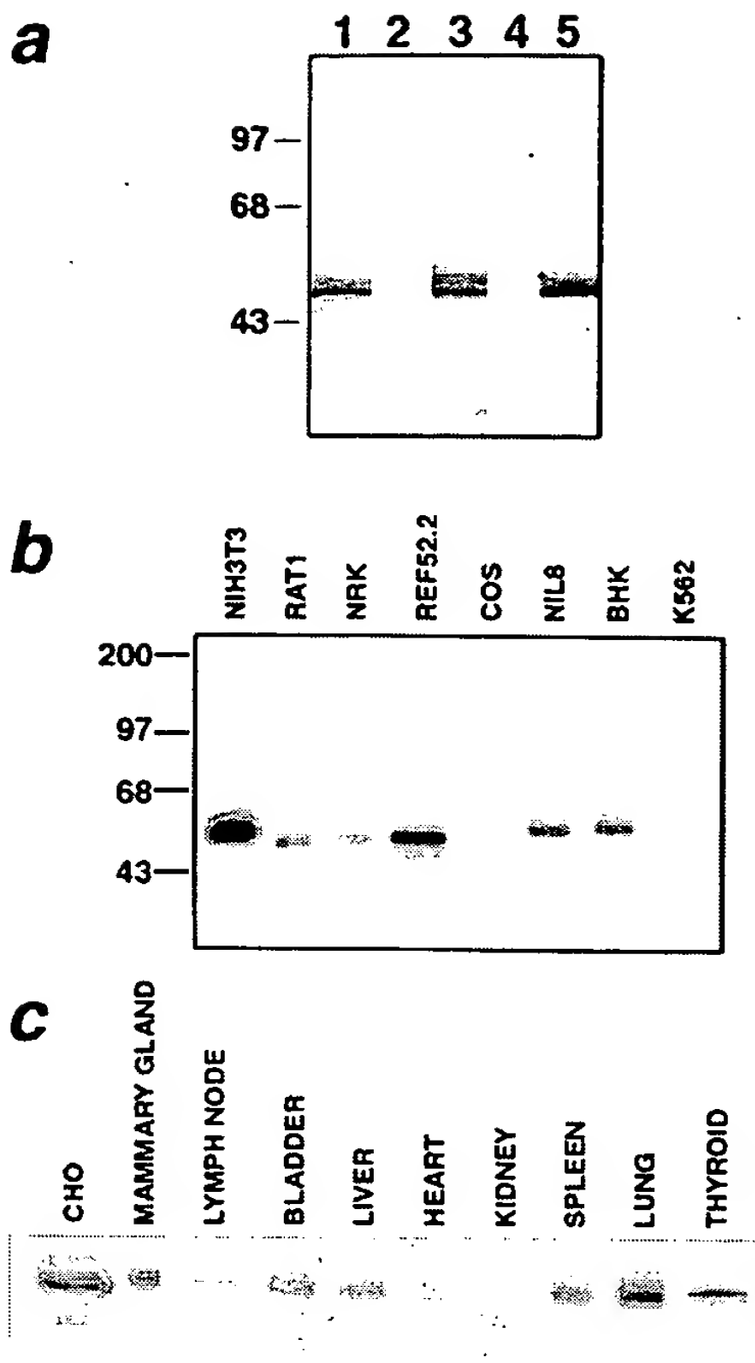

Figure 3. Expression of layilin protein in cells and tissues. (*a*) A rabbit polyclonal antiserum was raised against a synthetic peptide comprising the COOH-terminal 20 amino acids of layilin and used to Western blot a lysate of CHO cells. Lane *1*, immune serum; lane *2*, immune serum preincubated with 1 mg/ml layilin peptide; lane *3*, immune serum; lane *4*, immune serum after depletion over immobilized layilin peptide; lane *5*, affinity-purified antibody eluted from the immobilized layilin peptide. The position and size in kilodaltons of molecular weight standards are shown. (*b*) Western blot with affinity-purified anti-layilin antiserum of mouse, rat, monkey, hamster, and human cell lines. Specifically reacting bands in rat cell lines migrate slightly faster than do the prevalent immunoreactive species in monkey, mouse and hamster. NRK, normal rat kidney; REF, rat embryo fibroblast. The position and size in kD of molecular weight standards are shown. 5 μg of lysate were loaded per lane. (*c*) Organs were dissected from a healthy adult female mouse, homogenized, and lysed in gel-loading buffer. 10 μg of each lysate were loaded per lane, and were blotted for layilin. Total CHO protein is included to indicate the position of layilin.

proteins containing either talin or layilin sequences to bind layilin or talin, respectively, in detergent extracts from CHO cells. In each experiment, samples were assayed by Coomassie staining to ensure equal loading of GST fusion proteins. GST-layilin fusions containing amino acids 261–374 and 330–374 of the layilin cytoplasmic domain retained a fraction of intact talin in CHO detergent lysates, whereas a GST-layilin fusion containing amino acids 244–335 and a negative control GST-fusion containing a fibronectin type III repeat (GST-FN EIIIB) did not (Fig. 4 *a*). Moreover, the GST-layilin fusions distinguished between the full-length talin protein and a prominent proteolytic fragment present in the lysate by binding to only the full-length talin polypeptide. These observations indicate that the minimal talin binding site is within amino acids 330–374. This region of layilin includes three copies of the motif ESG(F/W)V (LH2) and two N(D/E)IY repeats (LH3), with each LH3 repeat adjacent to an LH2 repeat (Fig. 2 *a*). Talin binds to a GST fusion protein containing 1 or 3 copies of a tandem array of the LH2+LH3 repeats found at amino acids 243–252 of layilin (Fig. 4 *a* and data not shown). In addition, a synthetic peptide (LC20) derived from the COOH-terminal 20 amino acids of layilin and containing one copy of the LH2+LH3 module, blocks binding of talin to GST-layilin 330–374 (Fig. 4 *a*). In contrast to LC20, an unrelated peptide containing the HA epitope does not block binding of talin to the GST-layilin fusion protein (Fig. 4 *a*). These observations confirm that talin binds layilin through one or more LH23 motifs.

Fig. 4 *b* (*bottom*) shows that glutathione-agarose preloaded with a GST fusion protein containing amino acids 1–435 of talin (GST-CT 1–435), the same talin fragment used in our LexA-talin head bait, binds layilin in CHO extracts, whereas glutathione-agarose loaded with equal amounts of a control GST-fibronectin fusion protein does not. The GST-CT fusion also binds HA-tagged layilin in extracts prepared from NIL8 cells expressing epitope-tagged layilin. Using the monoclonal 12CA5 to detect the epitope tag, we found that GST-talin fusions that include amino acids 280–435 can specifically retain HA-tagged layilin from a cell lysate (Fig. 4 *c*).

We used our GST-talin fusion protein to determine if other focal contact proteins bound to talin head. We examined the material bound to the talin and control fibronectin GST-fusions for the presence of other focal contact proteins, and found that FAK bound to talin's NH_2-terminal domain (Fig. 4 *b*, *top*). This confirms and extends previous reports of an interaction between FAK and talin (Chen et al., 1995; Zheng et al., 1998). We did not detect any binding of α-actinin, vinculin, tensin, paxillin, tubulin, or β1-integrin to GST-CT 1–435 or to GST-FN EIIIB (data not shown). We used this assay to map the sequences within talin head sufficient for layilin and FAK binding (Fig. 4, *b* and *c*). Layilin bound to each GST-talin fusion containing at least amino acids 280–435. FAK bound well to GST-fusions that include amino acids 186–435. Shorter fusions overlapping amino acids 225–357 and a fusion protein containing only amino acids 225–357 of talin bound FAK weakly. Hence, amino acids 225–357 contain a minimal FAK-binding site, and amino acids 280–435 constitute the smallest layilin-binding site tested. The FAK binding site maps entirely within talin's band 4.1 homologous domain, and the layilin-binding site overlaps this region while including more COOH-terminal talin sequences. The fact that these binding sites are distinguishable confirms the specificity of each interaction.

Layilin is a Glycoprotein Expressed on the Cell Surface

The presence of a putative signal sequence and transmembrane domain suggested that layilin would be found on the

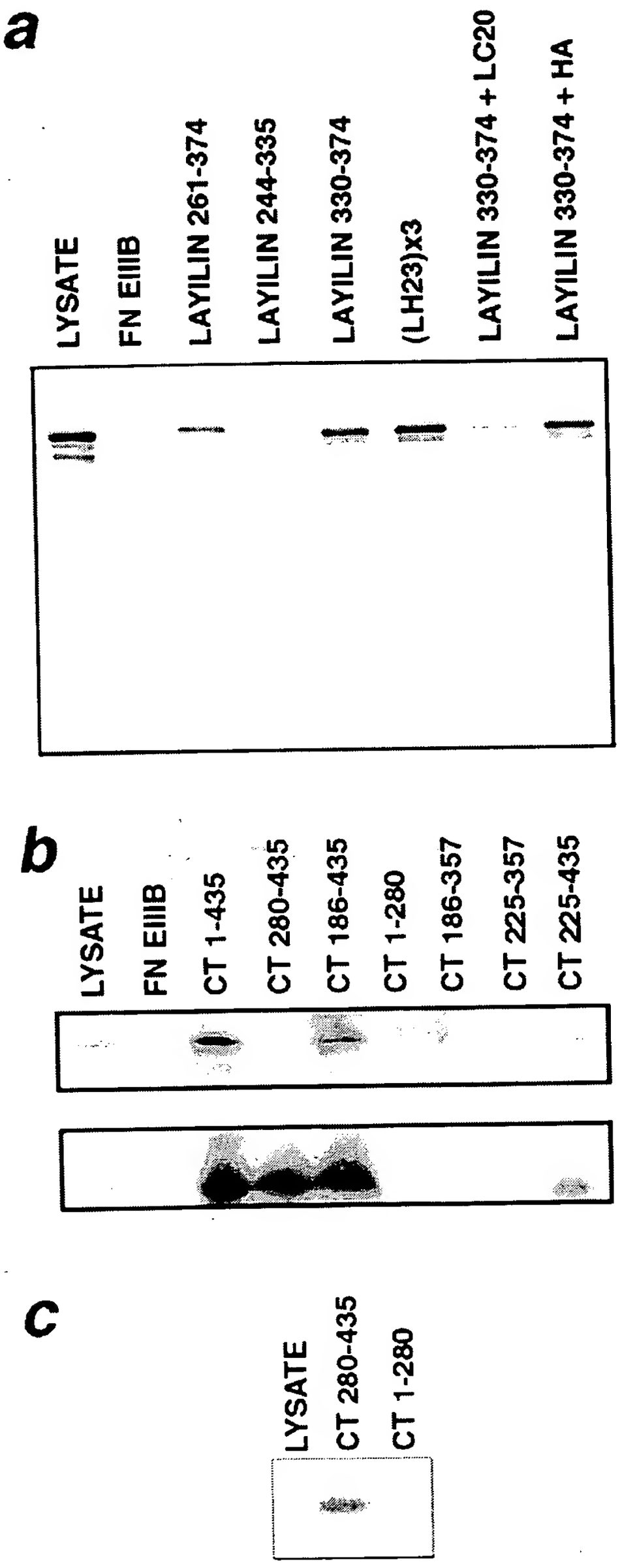

Figure 4. (*a*) GST fusion proteins containing portions of the layilin cytoplasmic domain were immobilized on agarose and mixed with a CHO cell detergent lysate. Each fusion protein contains the layilin amino acids indicated, except (LH23)×3, which has three copies of the amino acid motif spanning layilin amino acids 243–252. After washing, the agarose beads were boiled in gel-loading buffer, and the released material was analyzed by Western blotting for talin. The lanes containing proteins bound by GST fusions of fibronectin EIIIB (FN EIIIB) or layilin are overloaded approximately 13-fold relative to the total lysate lane. (*b*) Glutathione agarose preloaded with GST fusions containing either FN EIIIB or the indicated amino acids of chicken talin was incubated with a CHO cell detergent lysate, washed, and boiled in gel-loading buffer. Proteins released from the beads were detected by Western blotting for focal adhesion kinase (FAK, *top*) or layilin (*bottom*). The lanes containing proteins bound by GST fusions to chicken talin and fibronectin EIIIB are overloaded approximately 25-fold relative to the total lysate lane. (*c*) Glutathione agarose preloaded with GST fusions containing various fragments of chicken talin was incubated with a detergent lysate of NIL8 cells expressing HA-tagged layilin, washed, and boiled in gel-loading buffer. Proteins released from the beads were detected by Western blotting for the HA-epitope tag. Lanes containing material bound to GST fusions are overloaded approximately 20-fold relative to the total lysate lane.

cell surface. We tested this hypothesis by immunoprecipitation from surface-labeled CHO cell lysates. The anti-layilin antiserum immunoprecipitates from lysates of surface-biotinylated CHO cells a 55-kD band whose size is in good agreement with the band we detected by Western blotting of whole cell lysates with the same antibody (Fig. 5 *a*, lane *3*; Fig. 3 *a*, lanes *1*, *3*, and *5*; similar results were obtained with NIL8 hamster fibroblasts, data not shown). Peptide-depleted serum does not immunoprecipitate any surface-labeled material from biotin-labeled CHO cells, and the 55-kD band precipitated by the antiserum can be competed by preincubating the affinity-purified antiserum with a layilin-derived peptide (Fig. 5 *a*, lane *1*, and data not shown). We found that the surface-labeled band immunoprecipitated by anti-layilin antiserum is sensitive to treatment with PNGase F, indicating the presence of N-linked carbohydrates (Fig. 5 *a*, compare lanes *3* and *4*; Maley et al., 1989). The anti-HA epitope monoclonal 12CA5 immunoprecipitates a similarly sized, surface-labeled, PNGase F–sensitive band from both CHO and NIL8 cells expressing HA-tagged layilin (data not shown). Western blotting of CHO cell lysates treated with PNGase F shows a similar shift in the mobility of the band detected by anti-layilin antiserum, confirming that we are observing the same band by both surface label and Western blotting, and indicating that most of the cellular pool of layilin is glycosylated (Fig. 5 *b*). PNGase F-treated layilin migrates slightly slower than predicted based on its deduced amino acid sequence (51 vs. 43 kD); this discrepancy may reflect additional posttranslational modifications to layilin, such as O-linked glycosylation, or may simply reflect aberrant electrophoretic migration.

We used accessibility to a membrane nonpermeable biotinylation reagent to assess the proportion of total layilin present on the cell surface. A population of CHO cells was divided into two parts: one was surface-labeled with sulfo-NHS-LC-biotin while the other was subjected to the same surface-labeling protocol in parallel without adding biotin. Lysates made from these two samples were applied to identical columns of immobilized avidin to capture any proteins that reacted with the surface-labeling reagent,

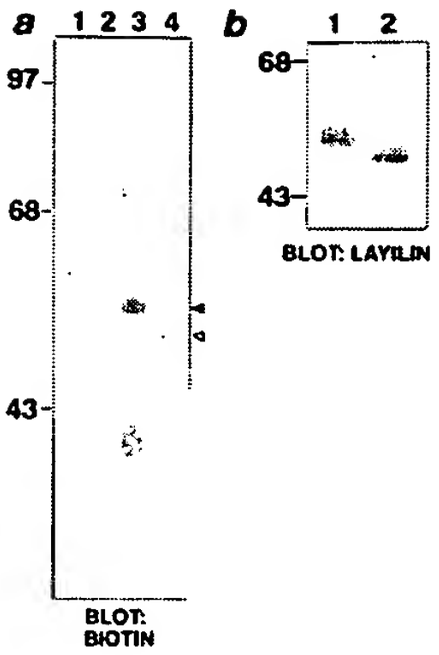

Figure 5. Layilin is a glycoprotein expressed on the cell surface. (*a*) CHO cells were surface-labeled with biotin, lysed in RIPA buffer, immunoprecipitated with either peptide-depleted (lanes *1* and *2*) or affinity-purified (lanes *3* and *4*) anti-layilin antiserum, and labeled bands were detected with HRP-streptavidin. Samples in lanes *2* and *4* were treated with PNGase F to remove N-linked carbohydrates. The position of the layilin band is marked with a solid arrowhead before PNGase F treatment, and with an open arrowhead after PNGase F treatment. The position and size in kD of molecular mass standards are shown. (*b*) A detergent lysate of CHO cells was treated with (lane *2*) or without (lane *1*) PNGase F to remove N-linked sugars, Western-blotted, and probed with affinity-purified anti-layilin antiserum. Note that essentially all the layilin present in the lysate is PNGase F-sensitive. The position and size in kD of molecular weight standards are shown. (*c*) Layilin is predominantly found on the cell surface. CHO cells were surface-labeled with biotin (lanes *2–4*) or mock surface-labeled without biotin (lanes *5–7*), lysed, and passed over an avidin column to remove labeled material. The first three fractions eluted from each column (lanes *2–4* and *5–7*) were analyzed by Western blotting for β1-integrin and layilin. When assayed for β1-integrin (*top*), the lysate (lane *1*) contains two bands: the upper band (*arrow*) represents mature β1-integrin; the lower band (*asterisk*) is an intracellular precursor. Biotin selectively labels the mature (*top*) band without affecting the precursor form of β1 (compare lanes *2* and *5*, *top*), indicating the reagent does not have access to the cells' interior. The same fractions (*bottom*) reveal that most layilin, like mature β1-integrin, is biotin-labeled (compare lanes *2* and *5*, *bottom*). All lanes were loaded with equivalent fractions of the cell lysate.

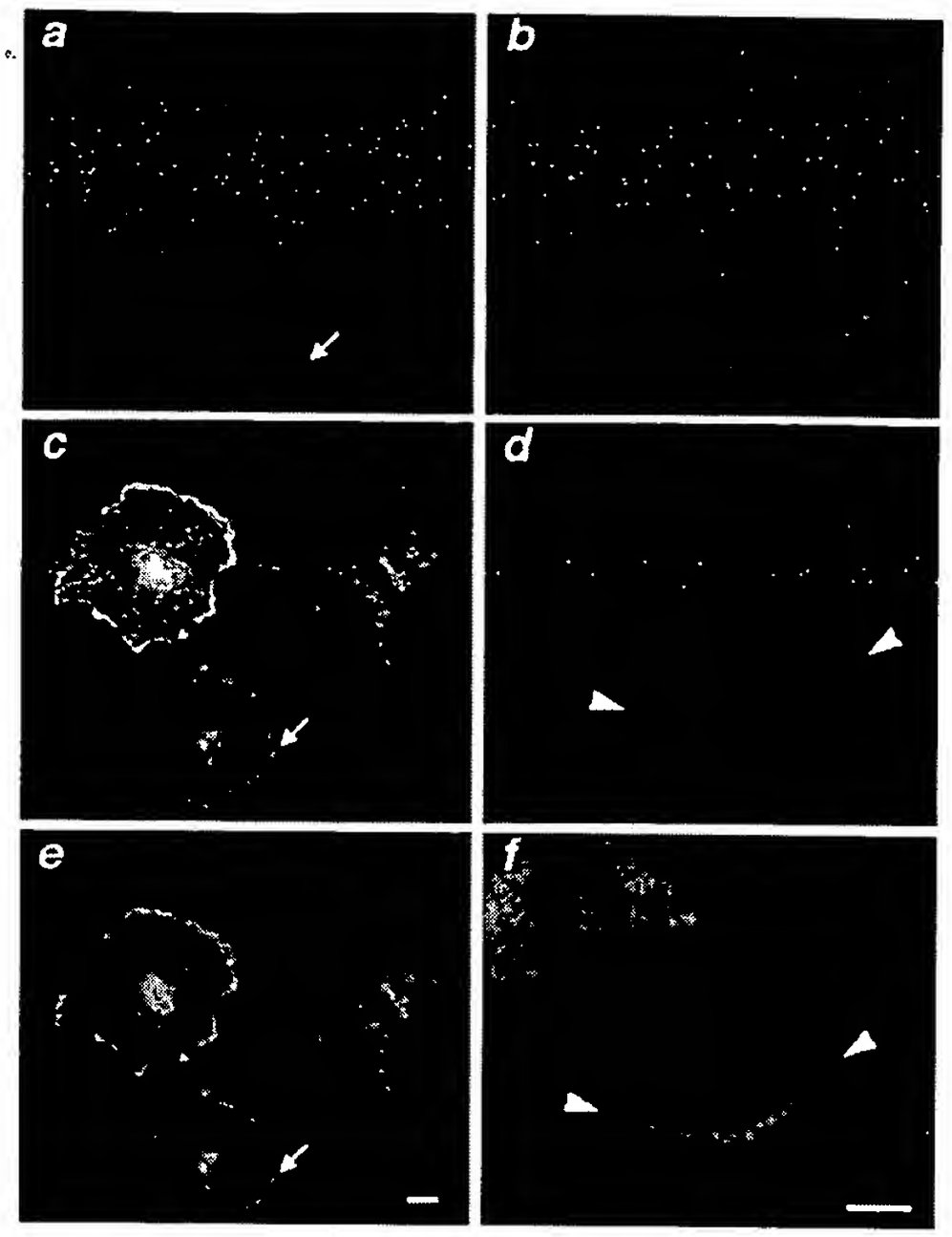

Figure 6. Localization of HA-tagged layilin in spreading (*a*, *c*, and *e*) or migrating (*b*, *d*, and *f*) NIL8 hamster cells. Cells spreading on a fibronectin matrix (*a*, *c*, and *e*) contain peripheral ruffles that stain for both HA-layilin (*a*) and phalloidin (*e*). Yellow ruffles in the double exposure (*c*) show the extent of overlap of staining. Migrating NIL8 cells also contain layilin-rich ruffles at their leading edges (*b*, *d*, and *f*). Cells shown are stained with 12CA5 in the presence of 1 mg/ml LC20 (*b*), 12CA5 in the presence of 1 mg/ml HA peptide (*d*), and the same cell as in *d* double-stained with affinity-purified anti-layilin antiserum (*f*). Bar, 10 μm.

thereby depleting surface proteins from the extracts. The flow-throughs from these columns were then analyzed by Western blotting for β1-integrin and layilin (Fig. 5 *c*). The integrin control indicates that the avidin column efficiently removed all of the mature surface-expressed β1-integrin (Fig. 5 *c*, *arrow*) from the labeled lysates (lanes *2–4*) without affecting the amount of precursor β1-integrin (which is not expressed on the surface; Fig. 5 *c*, *asterisk*). In contrast, the avidin column did not deplete either form of β1-integrin from mock-labeled lysates (Fig. 5 *c*, lanes *5–7*). By assaying the same fractions for layilin, we found that the majority of layilin was depleted in the biotin-treated sample when compared with the unbiotinylated control, indicating that most layilin protein is on the cell surface (Fig. 5 *c*, *bottom*; compare lanes *2–4* with lanes *5–7*).

Layilin Localization

We chose to analyze layilin subcellular distribution in NIL8 hamster fibroblasts because they have a well-articulated actin cytoskeleton that has been extensively characterized (Mautner and Hynes, 1977; Hynes and Destree, 1978). To confirm the specificity of our observations, we examined the distribution of both HA-tagged and endogenous layilin. In NIL8 cells stably transfected with an HA epitope–tagged version of layilin, 12CA5, the monoclonal antibody directed against the HA epitope tag, stains ruffling membranes in both spreading and migrating cells (Fig. 6, *a–f*). 15 min after plating on fibronectin-coated coverslips, NIL8 cells have a rim of F-actin filaments around the cell edge (Fig. 6 *e*). Spreading cells expressing HA-tagged layilin exhibit strong staining that colocalizes with phalloidin signal at the cell periphery (Fig. 6, *a*, *c*, and *e*). As an internal control, we examined nonexpressing cells in the same field; these cells have ruffles as assessed by phalloidin staining, but show no 12CA5 signal in the ruffles, indicating that 12CA5 staining produces little or no background in NIL8 cells (Fig. 6, *a*, *c*, and *e*, *arrows*).

The leading edges of migrating cells also contain actin- and talin-rich ruffles. To assess layilin localization in these

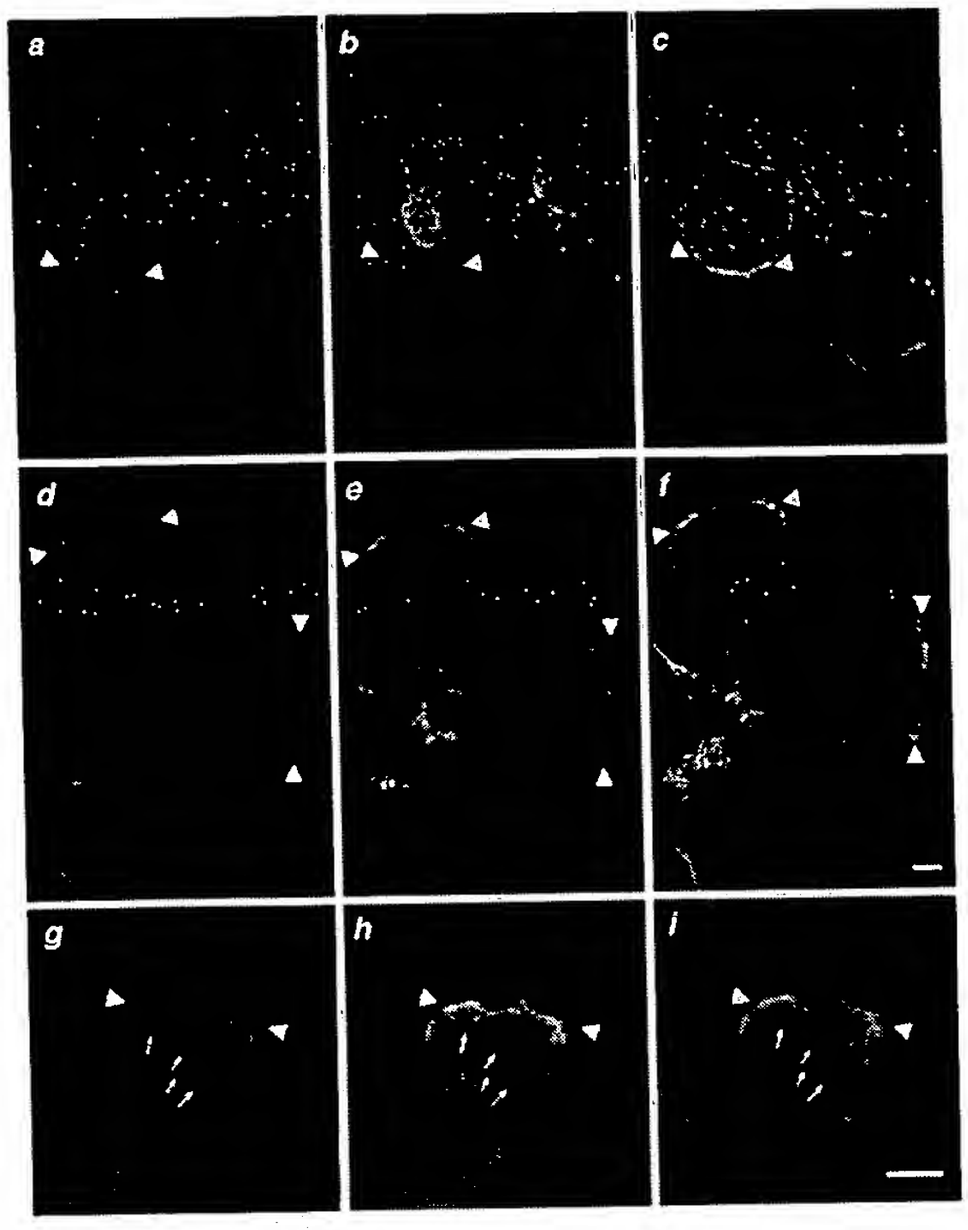

Figure 7. Endogenous layilin is in membrane ruffles. Cells are shown stained with peptide-depleted anti-layilin antiserum (*a*), affinity-purified anti-layilin antiserum (*d* and *g*), phalloidin (*c* and *f*), and anti-talin (*i*). *b*, *e*, and *h* are double exposures of *a* and *c*, *d* and *f*, and *g* and *i*. Layilin antibodies stain membrane ruffles (*arrowheads*) which also contain talin (*i*) and actin (*f*). The talin monoclonal stains both ruffles (*h* and *i*, *arrowheads*) and focal contacts (*h* and *i*, *arrows*), while the layilin antiserum stains ruffles but not focal contacts (*g* and *h*). Bar, 10 μm.

ruffles, we stimulated cells to migrate by wounding confluent monolayers with a rubber cell scraper, and examined the distribution of epitope-tagged layilin in cells migrating into the wound. 45–90 min after wounding, we observed lamellipodia with phase-dark ruffles on 10–30% of cells adjacent to the region cleared of cells. We detected HA-tagged layilin in these leading edge ruffles formed by migrating cells (Fig. 6, *b*, *d*, and *f*). This HA signal is competed by a peptide containing the HA epitope, but not by an unrelated peptide (LC20), demonstrating the specificity of the observed staining (Fig. 6, *b* and *d*). The cell in Fig. 6 *d* is double-stained with the polyclonal anti-layilin antiserum in Fig. 6 *f* to show that the cell has a layilin-positive ruffle at its leading edge.

We next examined the distribution of endogenous layilin in untransfected NIL8 cells. Our affinity-purified polyclonal anti-layilin antiserum stains the leading edge of migrating cells and peripheral ruffles of spreading cells (Fig. 7). Signals in the nucleus and the midbody are probably artifacts of the antiserum as we saw no nuclear or midbody staining with 12CA5 in cells expressing HA-tagged layilin (Fig. 6 and data not shown). Furthermore, our biochemical analysis, which suggests that layilin is predominantly on the cell surface, is inconsistent with the presence of significant levels of layilin in the nucleus (Fig. 5 *c*).

We compared the distribution of endogenous layilin with that of F-actin in NIL8 cells that were grown overnight on fibronectin-coated coverslips. The cell shown in Fig. 7, *d–f* is extending two lamellipodia at right angles to one another, each showing strong layilin staining at its leading edge. Phalloidin staining confirms that F-actin is also concentrated in these structures (Fig. 7 *f*). The cell shown in Fig. 7, *d–f*) has recently divided, and has not yet formed actin stress fibers characteristic of a well-spread cell. However, we did not observe specific stress-fiber staining with the anti-layilin antiserum in well-spread cells exhibiting prominent stress fibers (data not shown). Control anti-layilin antiserum was depleted of layilin immunoreactivity by preincubation of immune serum on a column containing immobilized layilin peptide (Fig. 3 *a*). In contrast to the affinity-purified anti-layilin antiserum, the depleted serum does not stain peripheral actin-rich ruffles (Fig. 7, *a–c*).

Colocalization of Layilin with Talin in Ruffles

We used double-label immunofluorescence to see whether layilin colocalizes with talin in focal contacts or membrane ruffles. We induced leading edges in NIL8 cells by scraping monolayer cultures. The resulting ruffles show strong staining with the anti-talin monoclonal TD77, confirming earlier reports of talin in ruffling membranes (Fig. 7 *i*; Burridge and Connell, 1983; DePasquale and Izzard, 1991; Bolton et al., 1997). In the same cells, talin is also readily seen in focal contacts arrayed behind the leading edge (Fig. 7, *h* and *i*, *arrows*). Layilin staining is clearly visible in the same ruffles that contain talin, but is not evident in focal contacts (Fig. 7 *g*, *arrows*). The coincidence of talin and layilin staining in these cells is indicated by yellow staining in the merged image of layilin and talin immunofluorescence, while the green focal contacts confirm that talin, but not layilin, is found in focal contacts (Fig. 7 *h*). Overall, we found essentially identical subcellular distribution in ruffles of both endogenous and HA-tagged layilin. The layilin signal colocalizes with both talin and phalloidin staining found in peripheral ruffles, but not with stress fibers or focal contacts (Fig. 7 and data not shown).

Discussion

Talin was discovered as a component of focal contacts and the leading edge of migrating cells, but the molecular basis of its role in ruffles is unknown (Burridge and Connell, 1983). Similarly, the significance of talin's band 4.1 homology, initially observed when the talin cDNA was reported (Rees et al., 1990), has not been revealed. The discovery of layilin, an integral membrane protein found in ruffles that binds to talin's band 4.1 homologous domain, confirms the hypothesis of Rees et al. that this domain of talin contains a membrane-binding site, and suggests a specific function for talin in the leading edge of migrating cells as an adaptor between the membrane and F-actin. A role for talin in migration was initially suggested by its subcellular localization in ruffles, and was demonstrated by the inhibitory

effect of microinjecting anti-talin antibodies into cells along the edge of a wound (Nuckolls et al., 1992; Bolton et al., 1997). Microinjecting a monoclonal antibody (TA205) that recognizes a fusion protein containing amino acids 139–433 within talin head domain also inhibits cell motility, further implicating this talin fragment in cell motility (Bolton et al., 1997). The monoclonal antibody TA205 recognizes a GST-talin fusion containing amino acids 1–186, placing the epitope between amino acids 139 and 186 (our unpublished observations); we have identified binding sites for both FAK and layilin adjacent to this antibody binding site, which may account for its inhibitory activity (Fig. 4). Talin's role in the dynamic aspects of membrane–cytoskeletal junctions in vertebrate cells is underscored by the observation that localized disruption of talin in neuronal growth cones prevents formation of new membrane extensions (Sydor et al., 1996). By binding to integrins and layilin, two types of transmembrane proteins with distinct subcellular distributions, talin may be able to distinguish between the relatively static membrane–cytoskeletal connections in focal contacts and the highly dynamic membrane–actin linkages in ruffles. How the talin–layilin interaction is regulated by or contributes to the control of membrane–cytoskeleton associations is the subject of ongoing investigations.

Models for Layilin Function

Given the colocalization of layilin with talin and the observed binding between them, layilin is a good candidate for a membrane-binding site for talin in ruffles. We observe colocalization of both epitope-tagged and endogenous layilin with talin in actin-rich membrane ruffles (Figs. 6 and 7). Bacterially expressed GST-talin fusion proteins bound layilin in cell lysates, and, in parallel experiments, GST-layilin cytoplasmic domain fusions bound talin in cell lysates (Fig. 4). These results, in addition to our initial finding that talin and layilin interact in a yeast two-hybrid assay, are consistent with a direct interaction between the two proteins. Layilin contains significant homology to proteins with C-type lectin activity. Carbohydrate recognition domains have been found in both type I (NH_2 terminus extracellular) and type II (NH_2 terminus cytoplasmic) single-pass transmembrane proteins (Drickamer and Taylor, 1993). Known type I C-type lectins fall into two functional groups: cell–cell adhesion molecules of the selectin family, and endocytic receptors such as the macrophage mannose receptor. This observation, combined with our initial characterization of the layilin protein, leads us to suggest two general models for layilin function.

In the first model, layilin acts in cell migration by anchoring to the membrane talin, which in turn binds F-actin. This chain of interactions may transmit force from actin to the membrane, resulting in its characteristic deformation into ruffles. In this scenario, layilin may serve simply as a talin docking site, or it could be an early-acting adhesion molecule that binds extracellular matrix, nucleating the formation of focal contact precursors at the cell periphery. In this case, layilin would be functioning analogously to selectins, which mediate transient adhesion between rolling leukocytes and the endothelium followed by tight integrin-mediated adhesion. However, whereas selectins mediate cell adhesion in specialized cells of the immune system, we hypothesize that layilin performs fundamental cell adhesion tasks common to most cells because layilin and talin are present in many different tissues (Fig. 3). Layilin would thus form transient adhesion sites between ruffles and extracellular matrix that are refined into focal contacts after integrin recruitment. This could occur in both spreading and migrating cells. Talin, which can bind both layilin and integrins, may provide continuity between the two types of cell–matrix linkages as transient layilin-containing structures mature into integrin-containing focal adhesions. Integrin extracellular matrix receptors are known to be signaling as well as adhesion receptors, and if layilin encounters matrix early in the process of cell adhesion it may also signal. The three internally repeated motifs in the layilin cytoplasmic domain are potential binding sites for cytoskeletal or signaling molecules in addition to talin. Conservation of these motifs in hamster and human layilins suggests that they are of importance, and we have shown that two of these repeats form a binding-site for talin (Fig. 4).

It is interesting to note that the C-type lectin CRD is structurally homologous to another carbohydrate-binding domain, the link module (Kohda et al., 1996). Link modules are found in a variety of carbohydrate-binding proteins, including CD44, one of the proteins reported to bind to the NH_2-terminal domain of ERMs (Tsukita et al., 1994). CD44 has also been proposed to function in cell migration and tumor metastasis (Sherman et al., 1994). It is notable that several members of the band 4.1 superfamily interact with the cytoplasmic domain of carbohydrate-binding molecules with roles in migration and adhesion.

In a second model, layilin may function as an endo- or phagocytic receptor, similar to some other C-type lectins such as the macrophage mannose receptor (Drickamer and Taylor, 1993). This model is suggested by the observation that talin is present in phagocytic cups in macrophages and at sites of uptake of some bacterial pathogens (Greenberg et al., 1990; Finlay et al., 1991; Finlay et al., 1992; Young et al., 1992; Love et al., 1998). In addition, the layilin cytoplasmic domain contains two YXXΦ motifs (YNVI, YDNM; Fig. 2 *a*). These motifs are similar to sequences that mediate clathrin-dependent endocytosis of other membrane proteins by binding to the μ2 chain of the AP-2 adaptor complex (Ohno et al., 1995; Marks et al., 1997). Layilin may act simply by binding to and internalizing ligands bearing an appropriate carbohydrate moiety, or it may have additional functions in recruitment or stabilization of cytoskeleton in phagocytic ruffles. Alternatively, talin might stabilize a complex consisting of layilin and its bound ligand during uptake. Again, we would postulate that, given its widespread expression pattern in tissues, layilin participates in some general mode of uptake not limited to macrophages or other professional phagocytes. These two models, adhesion and uptake, are not mutually exclusive, however, and we are currently engaged in experiments to confirm or rule out either possibility.

Implications for the Band 4.1 Superfamily

The band 4.1 superfamily members merlin and ezrin/radixin/

moesin are present in membrane ruffles, and downregulation of ERM proteins by treating cells with antisense oligonucleotides results in reduced cell adhesion (Takeuchi et al., 1994; Henry et al., 1995). This defect may be causal or may be a secondary consequence of reduced cell spreading. We are investigating the possible interaction of layilin with ERM proteins and other members of the band 4.1 superfamily found in ruffles. Previous reports of binding between band 4.1 family members and membrane proteins implicate clustered basic residues as binding sites for band 4.1 and ERMs. Jöns and Drenckhahn (1992) found that band 4.1 binds to the basic sequence LRRRY in the cytoplasmic domain of the erythrocyte anion exchanger, one band 4.1 membrane docking site in red blood cells. Marfatia and colleagues showed that mutation of three membrane-proximal basic residues in the glycophorin C cytoplasmic domain abrogates binding in vitro between protein 4.1 and peptides derived from glycophorin C (Hemming et al., 1995; Marfatia et al., 1995). Recently, Yonemura et al. (1998) identified short basic sequences in CD44, CD43, and ICAM-2 that appear to mediate binding to ERM proteins (Legg and Isacke, 1998; Yonemura et al., 1998). Interestingly, as shown in Fig. 4, talin binds to ten amino acids derived from two repeated motifs within the layilin cytoplasmic domain. This binding site does not contain the membrane proximal or any other stretch of basic residues in layilin, demonstrating another mode of binding between band 4.1 family members and integral membrane proteins.

The interaction of band 4.1 with glycophorin C is enhanced in the presence of polyphosphoinositides (Anderson and Marchesi, 1985). A mechanism for this regulation is suggested by studies on ERM proteins demonstrating binding between ERM head and tail domains that is reversed in the presence of acidic phospholipids (Gary and Bretscher, 1995; Magendantz et al., 1995; Hirao et al., 1996). Although no such regulated head–tail interaction has been described for talin, talin's NH_2-terminal domain has been reported to bind some phospholipids under conditions of low ionic strength (Niggli et al., 1994). In addition, talin undergoes a conformational change from a globular structure to an elongated rod in response to changes in salt concentration, which may represent a transition from a closed to an open form of the protein with different abilities to bind talin-binding partners (Molony et al., 1987; Winkler et al., 1997). We would have circumvented this mode of regulation with our recombinant LexA- and GST-fusion proteins that contain only talin head. Recent reports that ERM localization and head–tail association can be influenced by phosphorylation of ERMs suggest a potential mode of talin regulation that is consistent with observed talin phosphorylation (Pasquale et al., 1986; Turner et al., 1989; Beckerle, 1990; Bertagnolli et al., 1993; Tidball and Spencer, 1993; Matsui et al., 1998; Shaw et al., 1998). It will be of interest to determine whether talin binding to layilin or FAK is regulated by either phospholipid binding or talin phosphorylation.

In conclusion, we have uncovered novel functions for the talin head domain analogous with those of the homologous NH_2-terminal domains of other band 4.1 family members: interaction with layilin in ruffles, and FAK binding. This talin domain therefore acts both as a membrane linker and in signal transduction, while the tail of talin binds a different membrane anchor (integrins) and forms links to the cytoskeleton.

We wish to thank the Brent, Prasad, Krieger, Kaiser, and Weinberg labs for providing valuable two-hybrid materials. We are grateful to Michael DiPersio for providing the talin-head subclones A14 and GST-CT 1–435, and to David Critchley for providing the monoclonal antibodies TD77 and TA205. Thanks to Ed Clark, Michael DiPersio, Sheila Francis, and Frank Solomon for their insightful comments on the manuscript.

This work was supported by a grant from the National Cancer Institute (RO1 CA17007) and by the Howard Hughes Medical Institute. M. Borowsky received support from an NIGMS Predoctoral Training Grant to the Massachusetts Institute of Technology Biology Department, and R.O. Hynes is an Howard Hughes Medical Institute Investigator.

Received for publication 20 June 1998 and in revised form 1 September 1998.

References

Albigès-Rizo, C., P. Frachet, and M.R. Block. 1995. Down regulation of talin alters cell adhesion and the processing of the α5β1 integrin. *J. Cell Sci.* 108: 3317–3329.

Algrain, M., O. Turunen, A. Vaheri, D. Louvard, and M. Arpin. 1993. Ezrin contains cytoskeleton and membrane binding domains accounting for its proposed role as a membrane-cytoskeleton linker. *J. Cell Biol.* 120:129–139.

Alwine, J.C., D.J. Kemp, and G.R. Stark. 1977. Method for detection of RNAs in agarose gels by transfer to diazobenzyloxymethyl-paper and hybridization with DNA probes. *Proc. Natl. Acad. Sci. USA.* 74:5350–5354.

Anderson, R.A., and V.T. Marchesi. 1985. Regulation of the association of membrane skeletal protein 4.1 with glycophorin by a polyphosphoinositide. *Nature.* 318:295–298.

Beckerle, M.C. 1990. The adhesion plaque protein, talin, is phosphorylated in vivo in chick embryo fibroblasts exposed to a tumor-promoting phorbol ester. *Cell Regul.* 1:227–236.

Bennett, V. and D.M. Gilligan. 1993. The spectrin-based membrane skeleton and micron-scale organization of the plasma membrane. *Annu. Rev. Cell Biol.* 9:27–66.

Bertagnolli, M.E., S.J. Locke, M.E. Hensler, P.F. Bray, and M.C. Beckerle. 1993. Talin distribution and phosphorylation in thrombin-activated platelets. *J. Cell Sci.* 106:1189–1199.

Bolton, S.J., S.T. Barry, H. Mosley, B. Patel, B.M. Jockusch, J.M. Wilkinson, and D.R. Critchley. 1997. Monoclonal antibodies recognizing the N- and C-terminal regions of talin disrupt actin stress fibers when microinjected into human fibroblasts. *Cell Motil. Cytoskelet.* 36:363–376.

Bradley, J.E., G.A. Bishop, T. St. John, and J.A. Frelinger. 1988. A simple, rapid method for the purification of Poly A+ RNA. *Biotechniques.* 6:114–116.

Burn, P., A. Kupfer, and S.J. Singer. 1988. Dynamic membrane-cytoskeletal interactions: Specific association of integrin and talin arises in vivo after phorbol ester treatment of peripheral blood lymphocytes. *Proc. Natl. Acad. Sci. USA.* 85:497–501.

Burridge, K., and L. Connell. 1983. A new protein of adhesion plaques and ruffling membranes. *J. Cell Biol.* 97:359–367.

Burridge, K., and P. Mangeat. 1984. An interaction between vinculin and talin. *Nature.* 308:744–746.

Chen, H.-C., P.A. Appeddu, J.T. Parsons, J.D. Hildebrand, M.D. Schaller, and J.-L. Guan. 1995. Interaction of focal adhesion kinase with cytoskeletal protein talin. *J. Biol. Chem.* 270:16995–16999.

Chomczynski, P., and N. Sacchi. 1987. Single-step method of RNA isolation by acid guanidium thiocyanate-phenol-chloroform extraction. *Anal. Biochem.* 162:156–159.

DePasquale, J., and C. Izzard. 1991. Accumulation of talin in nodes at the edge of the lamellipodium and separate incorporation into adhesion plaques at focal contacts in fibroblasts. *J. Cell Biol.* 113:1351–1359.

Drickamer, K. 1992. Engineering galactose-binding activity into a C-type mannose-binding protein. *Nature.* 360:183–186.

Drickamer, K. 1993. Ca2+-dependent carbohydrate-recognition domains in animal proteins. *Curr. Opin. Struct. Biol.* 3:393–400.

Drickamer, K., and M.E. Taylor. 1993. Biology of animal lectins. *Annu. Rev. Cell Biol.* 9:237–264.

Espenshade, P., R. Gimeno, E. Holzmacher, P. Teung, and C. Kaiser. 1995. Yeast SEC16 gene encodes a multidomain vesicle coat protein that interacts with Sec23p. *J. Cell Biol.* 131:311–324.

Finlay, B.B., I. Rosenshine, M.S. Donnenberg, and J.B. Kaper. 1992. Cytoskeletal composition of attaching and effacing lesions associated with enteropathogenic *Escherichia coli* adherence to HeLa cells. *Infect. Immun.* 60: 2541–2543.

Finlay, B.B., S. Ruschkowski, and S. Dedhar. 1991. Cytoskeletal rearrangements accompanying *Salmonella* entry into epithelial cells. *J. Cell Sci.* 99:

283–296.
Gary, R., and A. Bretscher. 1995. Ezrin self-association involves binding of an N-terminal domain to a normally masked C-terminal domain that includes the F-actin binding site. *Mol. Biol. Cell.* 6:1061–1075.
Gilmore, A.P., C. Wood, V. Ohanian, P. Jackson, B. Patel, D.J.G. Rees, R.O. Hynes, and D.R. Critchley. 1993. The cytoskeletal protein talin contains at least two distinct vinculin binding domains. *J. Cell Biol.* 122:337–347.
Graves, B.J., R.L. Crowther, C. Chandran, J.M. Rumberger, S. Li, K.-S. Huang, D.H. Presky, P.C. Familletti, B.A. Wolitzky, and D.K. Burns. 1994. Insight into E-selectin/ligand interaction from the crystal structure and mutagenesis of the lec/EGF domains. *Nature.* 367:532–538.
Greenberg, S., K. Burridge, and S.C. Silverstein. 1990. Colocalization of F-actin and talin during Fc receptor-mediated phagocytosis in mouse macrophages. *J. Exp. Med.* 172:1853–1856.
Guo, Q., E. Vasile, and M. Krieger. 1994. Disruptions in golgi structure and membrane traffic in a conditional lethal mammalian cell mutant are corrected by ε-COP. *J. Cell Biol.* 125:1213–1224.
Gyuris, J., E.A. Golemis, H. Chertkov, and R. Brent. 1993. Cdi1, a human G1 and S phase protein phosphatase that associates with Cdk2. *Cell.* 75:791–803.
Helander, T.S., O. Carpen, O. Turunen, P.E. Kovanen, A. Vaheri, and T. Timonen. 1996. ICAM-2 redistributed by ezrin as a target for killer cells. *Nature.* 382:265–268.
Hemming, N.J., D.J. Anstee, M.A. Staricoff, M.J.A. Tanner, and N. Mohandas. 1995. Identification of the membrane attachment sites for protein 4.1 in the human erythrocyte. *J. Biol. Chem.* 270:5360–5366.
Hemmings, L., D.J.G. Rees, V. Ohanian, J.J. Bolton, A.P. Gilmore, B. Patel, H. Priddle, J.E. Trevithick, R.O. Hynes, and D.R. Critchley. 1996. Talin contains three actin-binding sites each of which is adjacent to a vinculin-binding site. *J. Cell Sci.* 109:2715–2726.
Henry, M.D., C. Gonzalez Agosti, and F. Solomon. 1995. Molecular dissection of radixin: distinct and interdependent functions of the amino- and carboxy-terminal domains. *J. Cell Biol.* 129:1007–1022.
Hirao, M., N. Sato, T. Kondo, S. Yonemura, M. Monden, T. Sasaki, Y. Takai, S. Tsukita, and S. Tsukita. 1996. Regulation mechanism of ERM (ezrin/radixin/moesin) protein/plasma membrane association: possible involvement of phosphatidylinositol turnover and rho-dependent signaling pathway. *J. Cell Biol.* 135:37–51.
Hoffman, C.S., and F. Winston. 1987. A ten-minute DNA preparation from yeast efficiently releases autonomous plasmids for transformation of *Escherichia coli*. *Gene.* 57:267–272.
Horwitz, A., K. Duggan, C. Buck, M.C. Beckerle, and K. Burridge. 1986. Interaction of plasma membrane fibronectin receptor with talin–a transmembrane linkage. *Nature.* 320:531–533.
Hynes, R.O., and A.T. Destree. 1978. Relationships between fibronectin (LETS protein) and actin. *Cell.* 15:875–886.
Isberg, R.R., and J.M. Leong. 1990. Multiple β1 chain integrins are receptors for invasin, a protein that promotes bacterial penetration into mammalian cells. *Cell.* 60:861–871.
Jöns, T., and D. Drenckhahn. 1992. Identification of the binding interface involved in linkage of cytoskeletal protein 4.1 to the erythrocyte anion exchanger. *EMBO (Eur. Mol. Biol. Organ.) J.* 11:2863–2867.
Knezevic, I., T.M. Leisner, and S.C.-T. Lam. 1996. Direct binding of the platelet integrin $\alpha_{IIb}\beta_3$ (GPIIb-IIIa) to talin. *J. Biol. Chem.* 271:16416–16421.
Kohda, D., C.J. Morton, A.A. Parkar, H. Hatanaka, F.M. Inagaki, I.D. Campbell, and A.J. Day. 1996. Solution structure of the link module: a hyaluronan-binding domain involved in extracellular matrix stability and cell migration. *Cell.* 86:767–775.
Kreitmeier, M., G. Gerisch, C. Heizer, and A. Muller-Taubenberger. 1995. A talin homologue of *Dictyostelium* rapidly assembles at the leading edge of cells in response to chemoattractant. *J. Cell Biol.* 129:179–188.
Lawson, M.A., and F.R. Maxfield. 1995. Ca2+- and calcineurin-dependent recycling of an integrin to the front of migrating neutrophils. *Nature.* 377:75–79.
Lee, J., and K. Jacobson. 1997. The composition and dynamics of cell-substratum adhesions in locomoting fish keratocytes. *J. Cell Sci.* 110:2833–2844.
Legg, J.W., and C.M. Isacke. 1998. Identification and functional analysis of the ezrin-binding site in the hyaluronan receptor, CD44. *Curr. Biol.* 8:705–708.
Letourneur, F., and R.D. Klausner. 1992. A novel di-leucine motif and a tyrosine-based motif independently mediate lysosomal targeting and endocytosis of CD3 chains. *Cell.* 69:1143–1157.
Love, D.C., M.M. Kane, and D.M. Mosser. 1998. *Leishmania amazonensis*: The phagocytosis of amastigotes by macrophages. *Exp. Parasitol.* 88:161–171.
Magendantz, M., M.D. Henry, A. Lander, and F. Solomon. 1995. Interdomain interactions of radixin in vitro. *J. Biol. Chem.* 270:25324–25327.
Maley, F., R.B. Trimble, A.L. Tarentino, and T.H. Plummner. 1989. Characterization of glycoproteins and their associated oligosaccharides through the use of endoglycosidases. *Anal. Biochem.* 180:195–204.
Marcantonio, E.E., and R.O. Hynes. 1988. Antibodies to the conserved cytoplasmic domain of the integrin β1 subunit react with proteins in vertebrates, invertebrates, and fungi. *J. Cell Biol.* 106:1765–1772.
Marfatia, S.M., R.A. Lue, D. Branton, and A.H. Chishti. 1995. Identification of the protein 4.1 binding interface on glycophorin C and p55, a homologue of the *Drosophila discs-large* tumor suppressor protein. *J. Biol. Chem.* 270:715–719.
Marks, M.S., H. Ohno, T. Kirchhausen, and J.S. Bonifacino. 1997. Protein sorting by tyrosine-based signals: adapting to the Ys and wherefores. *Trends Cell Biol.* 7:124–128.
Matsui, T., M. Maeda, Y. Doi, S. Yonemura, M. Amano, K. Kaibuchi, S. Tsukita, and S. Tsukita. 1998. Rho-kinase phosphorylates COOH-terminal threonines in ezrin/radixin/moesin (ERM) proteins and regulates their head-to-tail association. *J. Cell Biol.* 140:647–657.
Mautner, V., and R.O. Hynes. 1977. Surface distribution of LETS protein in relation to the cytoskeleton of normal and transformed cells. *J. Cell Biol.* 75: 743–768.
McLachlan, A.D., M. Stewart, R.O. Hynes, and D.J.G. Rees. 1994. Analysis of repeated motifs in the talin rod. *J. Mol. Biol.* 235:1278–1290.
Molony, L., D. McCaslin, J. Abernethy, B. Paschal, and K. Burridge. 1987. Properties of talin from chicken gizzard smooth muscle. *J. Biol. Chem.* 262: 7790–7795.
Moulder, G.L., M.M. Huang, R.H. Waterston, and R.J. Barstead. 1996. Talin requires β-integrin, but not vinculin, for its assembly into focal adhesion-like structures in the nematode *Caenorhabditis elegans*. *Mol. Biol. Cell.* 7:1181–1193.
Murthy, A., C. Gonzalez-Agosti, E. Cordero, D. Pinney, C. Candia, F. Solomon, J. Gusella, and V. Ramesh. 1998. NHE-RF, a regulatory cofactor for Na+-H+ exchange, is a common interactor for merlin and ERM (MERM) proteins. *J. Biol. Chem.* 273:1273–1276.
Niggli, V., S. Kaufmann, W.H. Goldmann, T. Weber, and G. Isenberg. 1994. Identification of functional domains in the cytoskeletal protein talin. *Eur. J. Biochem.* 224:951–957.
Nuckolls, G.H., L.H. Romer, and K. Burridge. 1992. Microinjection of antibodies against talin inhibits the spreading and migration of fibroblasts. *J. Cell Sci.* 102:753–762.
Nuckolls, G.H., C.E. Turner, and K. Burridge. 1990. Functional studies of the domains of talin. *J. Cell Biol.* 110:1635–1644.
Ohno, H., J. Stewart, M.-C. Fournier, H. Bosshart, I. Rhee, S. Miyatake, T. Saito, A. Gallusser, T. Kirchhausen, and J.S. Bonifacino. 1995. Interaction of tyrosine-based sorting signals with clathrin-associated proteins. *Science.* 269: 1872–1875.
Pasquale, E.B., P.A. Maher, and S.J. Singer. 1986. Talin is phosphorylated on tyrosine in chicken embryo fibroblasts transformed by Rous sarcoma virus. *Proc. Natl. Acad. Sci. USA.* 83:5507–5511.
Peters, J.H., J.E. Trevithick, P. Johnson, and R.O. Hynes. 1995. Expression of the alternatively spliced EIIIB segment of fibronectin. *Cell Adh. Comm.* 3:67–89.
Reczek, D., M. Berryman, and A. Bretscher. 1997. Identification of EBP50: a PDZ-containing phosphoprotein that associates with members of the ezrin-radixin-moesin family. *J. Cell Biol.* 139:169–179.
Rees, D.J.G., S.E. Ades, S.J. Singer, and R.O. Hynes. 1990. Sequence and domain structure of talin. *Nature.* 347:685–689.
Sambrook, J., E.F. Fritsch, and T. Maniatis. 1989. Molecular Cloning. Cold Spring Harbor Laboratory Press, Plainview, NY.
Schmidt, C.E., A.F. Horwitz, D.A. Lauffenburger, and M.P. Sheetz. 1993. Integrin-cytoskeletal interactions in migrating fibroblasts are dynamic, asymmetric, and regulated. *J. Cell Biol.* 123:977–991.
Serrador, J.M., J.L. Alonso-Lebrero, M.A. del Pozo, H. Furthmayr, R. Schwartz-Albiez, J. Calvo, F. Lozano, and F. Sánchez-Madrid. 1997. Moesin interacts with the cytoplasmic region of intercellular adhesion molecule-3 and is redistributed to the uropod of T lymphocytes during cell polarization. *J. Cell Biol.* 138:1409–1423.
Shaw, R.J., M. Henry, F. Solomon, and T. Jacks. 1998. RhoA-dependent Phosphorylation and relocalization of ERM proteins into apical membrane/actin protrusions in fibroblasts. *Mol. Biol. Cell.* 9:403–419.
Sherman, L., J. Sleeman, P. Herrlich, and H. Ponta. 1994. Hyaluronate receptors: key players in growth, differentiation, migration and tumor progression. *Curr. Opin. Cell Biol.* 6:726–733.
Sydor, A.M., A.L. Su, F.-S. Wang, A. Xu, and D.G. Jay. 1996. Talin and Vinculin Play Distinct Roles in Filopodial Motility in the Neuronal Growth Cone. *J. Cell Biol.* 134:1197–1207.
Takeuchi, K., N. Sato, H. Kasahara, N. Funayama, A. Nagafuchi, S. Yonemura, S. Tsukita, and S. Tsukita. 1994. Perturbation of cell adhesion and microvilli formation by antisense oligonucleotides to ERM family members. *J. Cell Biol.* 125:1371–1384.
Tapley, P., A. Horwitz, C. Buck, K. Duggan, and L. Rohrschneider. 1989. Integrins isolated from Rous sarcoma virus-transformed chicken embryo fibroblasts. *Oncogene.* 4:325–333.
Tidball, J.G., and M.J. Spencer. 1993. PDGF stimulation induces phosphorylation of talin and cytoskeletal reorganization in skeletal muscle. *J. Cell Biol.* 123:627–635.
Towbin, H., T. Staehelin, and J. Gordon. 1979. Electrophoretic transfer of proteins from polyacrylamide gels to nitrocellulose sheets: Procedure and some applications. *Proc. Natl. Acad. Sci. USA.* 76:4350–4354.
Tsukita, S., K. Oishi, N. Sato, J. Sagara, A. Kawai, and S. Tsukita. 1994. ERM family members as molecular linkers between the cell surface glycoprotein CD44 and actin-based cytoskeletons. *J. Cell Biol.* 126:391–401.
Tsukita, S., S. Yonemura, and S. Tsukita. 1997. ERM (ezrin/radxin/moesin) family: from cytoskeleton to signal transduction. *Curr. Opin. Cell Biol.* 9:70–75.
Turner, C.E., F.M. Pavalko, and K. Burridge. 1989. The role of phosphorylation and limited proteolytic cleavage of talin and vinculin in the disruption of focal adhesion integrity. *J. Biol. Chem.* 264:11938–11944.

Turunen, O., T. Wahlstrom, and A. Vaheri. 1994. Ezrin has a COOH-terminal actin-binding site that is conserved in the ezrin protein family. *J. Cell Biol.* 126:1445–1453.

Ungewickell, E., P.M. Bennett, R. Calvert, V. Ohanian, and W.B. Gratzer. 1979. In vitro formation of a complex between cytoskeletal proteins of the human erythrocyte. *Nature.* 280:811–814.

von Heijne, G. 1986. A new method for predicting signal sequence cleavage sites. *Nucleic Acids Res.* 14:4683–4690.

Weis, W.I., R. Kahn, R. Fourme, K. Drickamer, and W.A. Hendrickson. 1991. Structure of the calcium-dependent lectin domain from a rat mannose-binding protein determined by MAD phasing. *Science.* 254:1608–1615.

Wilson, I.A., H.L. Niman, R.A. Houghten, A.R. Cherenson, M.L. Connolly, and R.A. Lerner. 1984. The structure of an antigenic determinant in a protein. *Cell.* 37:767–778.

Winkler, J., H. Lunsdorf, and B. Jockusch. 1997. Energy-filtered electron microscopy reveals that talin is a highly flexible protein composed of a series of globular domains. *Eur. J. Biochem.* 243:430–436.

Yonemura, S., M. Hirao, Y. Doi, N. Takahashi, T. Kondo, S. Tsukita, and S. Tsukita. 1998. Ezrin/radixin/moesin (ERM) proteins bind to a positively charged amino acid cluster in the juxta-membrane cytoplasmic domain of CD44, CD43, and ICAM-2. *J. Cell Biol.* 140:885–895.

Young, V.B., S. Falkow, and G.K. Schoolnik. 1992. The invasin protein of *Yersinia enterocolitica*: Internalization of invasin-bearing bacteria by eukaryotic cells is associated with reorganization of the cytoskeleton. *J. Cell Biol.* 116: 197–207.

Zervos, A.S., J. Gyuris, and R. Brent. 1993. Mxi1, a protein that specifically interacts with Max to bind Myc-Max recognition sites. *Cell.* 72:223–232.

Zheng, C., X. Zheng, C.Z. Bian, C. Guo, A. Akbay, L. Warner, and J.-L. Guan. 1998. Differential regulation of Pyk2 and Focal Adhesion Kinase (FAK). *J. Biol. Chem.* 273:2384–2389.